

Inés Horovitz* and
Ross D. E.
MacPhee†

*Department of Vertebrate
Paleontology, American
Museum of Natural History,
New York, NY 10024-5192,
U.S.A. E-mail:

horovitz@amnh.org and

†Department of Mammalogy,
American Museum of Natural
History, New York, NY
10024-5192, U.S.A.

Received 23 February 1998
revision received 20 June
1998
and accepted 6 July 1998

Keywords: New World
monkeys, platyrrhines,
Antilles, Quaternary,
Antillothrix, *Xenothrix*,
Paralouatta, Caribbean.

The quaternary Cuban platyrrhine *Paralouatta varonai* and the origin of Antillean monkeys

We describe recently recovered dental and mandibular remains of the Cuban platyrrhine *Paralouatta varonai*, previously known from the holotype only (a nearly complete skull with very worn teeth). We also expand on the original description of the type specimen.

Paralouatta is one of three extinct taxa of Greater Antillean Quaternary monkeys known from craniodental remains. The other two, *Xenothrix mcgregori* and *Antillothrix bernensis*, occurred in Jamaica and Hispaniola, respectively. It has been common practice to assume that Antillean monkeys were more closely related to individual mainland taxa than to each other. Thus, *P. varonai* was thought to be related to *Alouatta*; *Antillothrix bernensis* to *Saimiri* or *Cebus*; and *X. mcgregori* to *Callicebus*, or to callitrichines, or even to be of unknown affinity. With the discovery of well-preserved dental remains of *Paralouatta*, it can now be ascertained that this species was in fact very different from *Alouatta*. Cladistic analysis reveals a sister-group relationship between *Antillothrix* and *Paralouatta*, followed on the cladogram by *Xenothrix* and *Callicebus* (last taxon being the closest mainland relative of the Antillean clade). This conclusion has an important biogeographic implication: recognition of an Antillean clade, as advocated here, assumes only one primate colonization from the South American mainland, not several as previously believed.

© 1999 Academic Press

Journal of Human Evolution (1999) 36, 33–68

Article No. jhev.1998.0259

Available online at <http://www.idealibrary.com> on **IDEAL**

Introduction

Platyrrhine primates have been a notable part of the mammalian fauna of South America since at least the late Oligocene/early Miocene (Hoffstetter, 1969; MacFadden, 1990). The living species are found from southern Mexico to northern Argentina, but the fossil record establishes the New World monkeys once ranged more widely, from Patagonia to the Greater Antilles (i.e., the island group consisting of Cuba, Hispaniola, Puerto Rico, and Jamaica). The past diversity of platyrrhines at the southern end of their distribution is becoming increasingly well known, thanks to more than a century of dedicated work in this region (Ameghino, 1906; Rusconi, 1934, 1935; Kraglievich, 1951; Hershkovitz, 1970, 1974, 1981,

1984; Fleagle & Bown, 1983; Fleagle *et al.*, 1987; Fleagle, 1990). By comparison, the diversity of the endemic platyrrhines of the Greater Antilles (hereafter, the Antillean monkeys) is known only in barest outline. The objective of this paper is to review recent progress in unravelling and interpreting the phylogeny of these monkeys, with particular emphasis on the late Quaternary species from Cuba, *Paralouatta varonai*.

Our understanding of the fossil history of Antillean monkeys may be getting broader in a geographical sense, but it is not very deep temporally. Cuba, Jamaica, and Hispaniola each supported one or more endemic platyrrhines during the late Quaternary, but Cuba is the only island with a Tertiary primate record—currently consisting of a single fossil, a talus of early Miocene

age from the important locality of Domo de Zaza (MacPhee & Iturralde-Vinent, 1995; Iturralde-Vinent & MacPhee, in press).

Fossils of extinct Antillean monkeys were found (although not properly recognized as such) as early as the 1920s in Hispaniola and Jamaica (MacPhee, 1996), but Williams & Koopman (1952) were responsible for shedding the first real light on the subject. Since then, a number of new discoveries have been made (Rimoli, 1977; Rosenberger, 1977; MacPhee & Woods, 1982; Ford & Morgan, 1988; Ford, 1990; Rivero & Arredondo, 1991; MacPhee *et al.*, 1995; MacPhee, 1996), but the Antillean record is still clouded by a variety of uncertainties. From a systematic standpoint, the most serious of these concerns how many species are actually represented in existing fossil assemblages, and how they are related to one another. There are three named taxa: *Paralouatta varonai* Rivero & Arredondo, 1991, from Cuba; *Xenothrix mcgregori* Williams & Koopman, 1952, from Jamaica; and *Antillothrix bernensis* MacPhee *et al.*, 1995 (formerly *Saimiri bernensis* Rimoli, 1977), from Hispaniola. There are, in addition, a number of primate-like postcranial remains from these islands that, for one reason or another, have not yet been allocated; some may represent unknown taxa (MacPhee & Fleagle, 1991; MacPhee, 1996). It is a safe bet that we are far from having a complete roster of Antillean monkeys, even for the Quaternary (Ford, 1990).

The relationships of Antillean monkeys are obscure. Indeed, until very recently, the only conclusion one could draw from the scanty literature on this subject was that these monkeys had little to do with one another. Thus, it might be concluded that Cuban *Paralouatta*, supposedly a close relative of *Alouatta* (Rivero & Arredondo, 1991), could not also be a near affine of Hispaniolan *Antillothrix bernensis* because the latter was viewed as either a giant squirrel

rel monkey (Rimoli, 1977) or some kind of cebine related to both *Saimiri* and *Cebus* (MacPhee & Woods, 1982). Similarly, it seemed unlikely that Jamaican *Xenothrix*, variously considered to be a callicebine, cebine, or a taxon of unknown affinities (Rosenberger, 1977; MacPhee & Fleagle, 1991), could be closely related to the monkeys from Cuba and Hispaniola. Adding to this already complex picture, Ford (1986a) and Ford & Morgan (1988) argued that several of the previously mentioned isolated postcranials from Hispaniola and Jamaica are specifically marmoset like, which implied that yet another major platyrrhine clade was once represented in the Greater Antilles.

It is self-evident that, if the primate complements of Cuba, Jamaica, and Hispaniola had multiple origins, there had to have been multiple colonization events. However, thanks to a number of new discoveries, especially ones made in the present decade, this picture of multiple separate colonizations by unrelated propagules is no longer so easily maintained. The multiple origins viewpoint was explicitly challenged by MacPhee *et al.* (1995), who demonstrated on the basis of a preliminary cladistic study that *Paralouatta* and *Antillothrix* are related as sister groups, and that *Callicebus* may be the closest living relative of this dyad. The position of *Xenothrix* was not investigated. However, it is of interest that Rosenberger (1977) independently posited that *Xenothrix* might be related to *Callicebus* on the basis of evidence then available. New fossils of *Xenothrix* (description of which is in preparation) provide an opportunity to determine whether all Antillean monkeys (or at least those represented by adequate material) may derive from a single colonizing ancestor.

One objective of this paper is to put on record a description and evaluation of all craniodental specimens of *P. varonai* so far recovered. Another is to present a comprehensive cladistic analysis of Antillean monkeys. We address the latter goal within

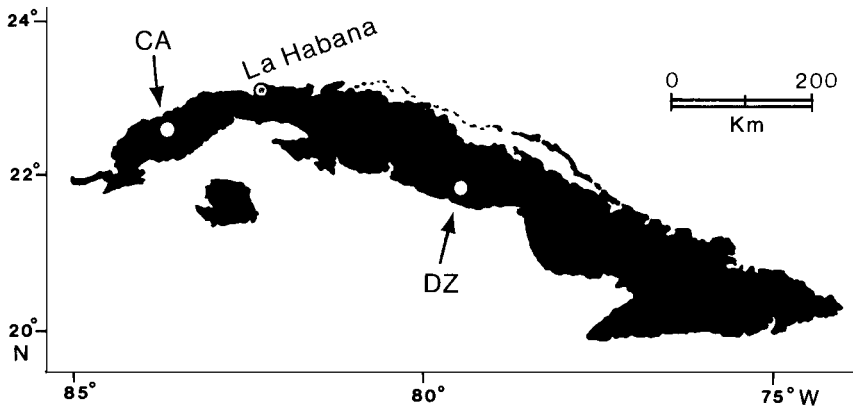


Figure 1. Map of Cuba showing principal localities: CA, Cueva Alta and Cueva del Mono Fósil (Quaternary); DZ, Domo de Zara (early Miocene).

the larger issue of platyrrhine systematics. To avoid ambiguity, in this paper we explicitly define pitheciins as including *Pithecia*, *Chiropotes*, and *Cacajao*, atelines as *Ateles*, *Brachyteles*, *Lagothrix*, and *Alouatta*, and callitrichines as *Callimico*, *Callithrix*, *Cebuella*, *Leontopithecus*, and *Saguinus*.

Abbreviations

AMNH,	American Museum of Natural History, New York
CMC,	Claremont-McKenna College, California
GPBSEC,	Grupo Espeleológico “Pedro Borrás” of the Sociedad Espeleológica de Cuba
MNHNH V,	Museo Nacional de Historia Natural, La Habana, Vertebrate Collection
M-D,	mesiodistal
B-L,	buccolingual

Craniodental morphology and relationships of *Paralouatta varonai*

Fossils allocated to *P. varonai* have been recovered at only two localities in Cuba, Cueva del Mono Fósil and nearby Cueva Alta (Rivero & Arredondo, 1991; Jáimez Salgado *et al.*, 1992). These sites are situ-

ated on the same south-facing slope of the Sierra de Galeras, one of several blocks of uplifted Jurassic limestones that make up the Cordillera de Guaniguanico (Figure 1).

The first primate fossils from Cueva del Mono Fósil were found in 1988 and included the type skull (Figure 2) and a distal humerus. Remains belonging to other vertebrates indicated that the temporal context of the site was Quaternary. The first detailed account of this material, by Rivero & Arredondo (1991), included a formal description of *P. varonai* and emphasized the similarity of the type skull to that of the living howler monkey, *Alouatta*.

Since the late 1980s, accessible portions of Cueva Alta and Cueva Mono Fósil have been carefully combed for new fossils by expeditions of the GPBSEC, MNHNH, and AMNH. A number of additional platyrrhine remains have been recovered as a result, including a mandible, numerous isolated teeth, and several postcranial pieces. Although exploration continues in the numerous caves that riddle the rest of the south face of Sierra de Galeras, to date no new primate-bearing fossil sites have been identified. This is, therefore, an opportune time to review, describe, and interpret what has been collected thus far.

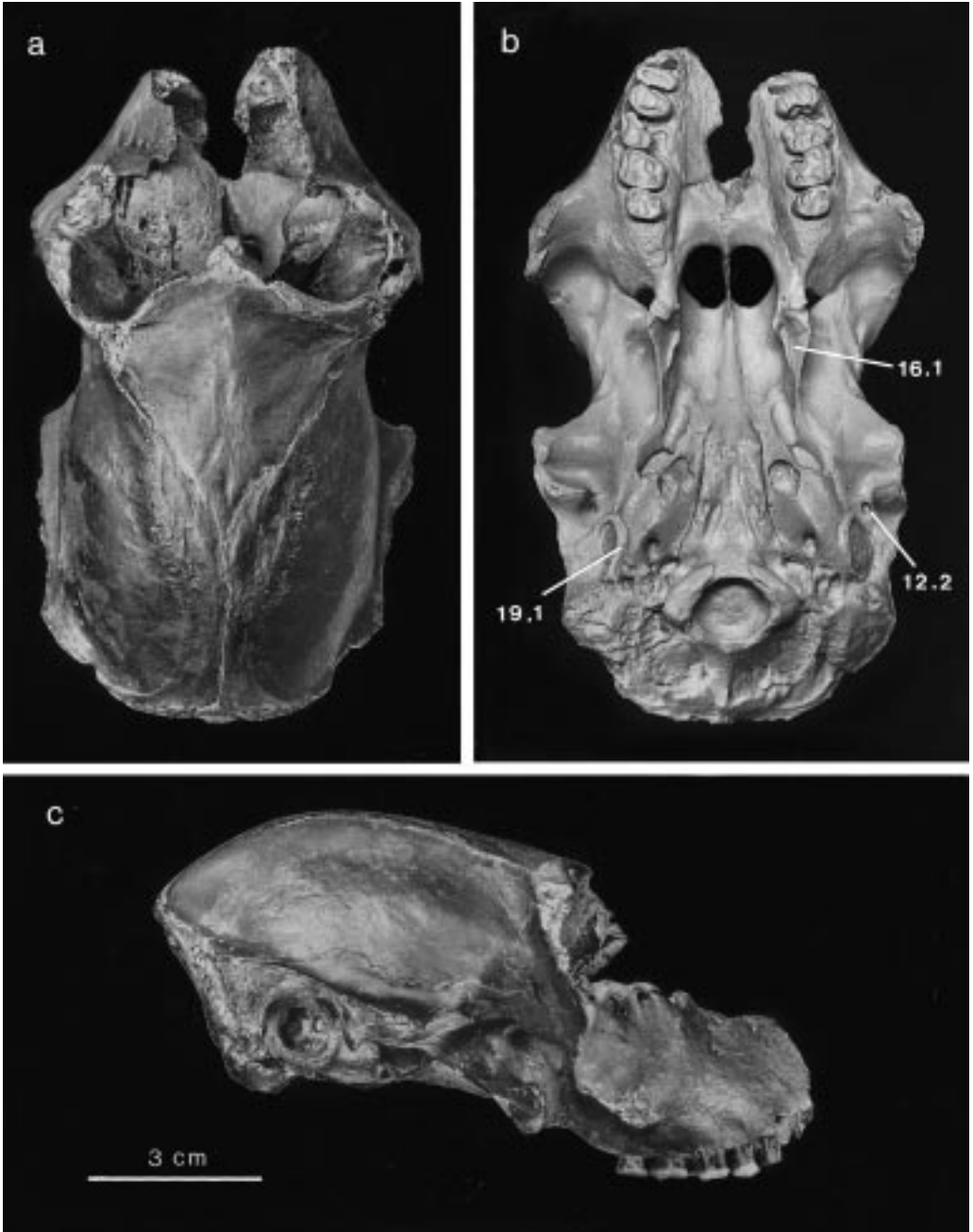


Figure 2.

Cueva del Mono Fósil and Cueva Alta are located on a *mogote* (a steep-walled limestone hill with a flat or gently rounded top).

It is now evident that most of the remains found in each cave did not occur there originally, but were brought down from

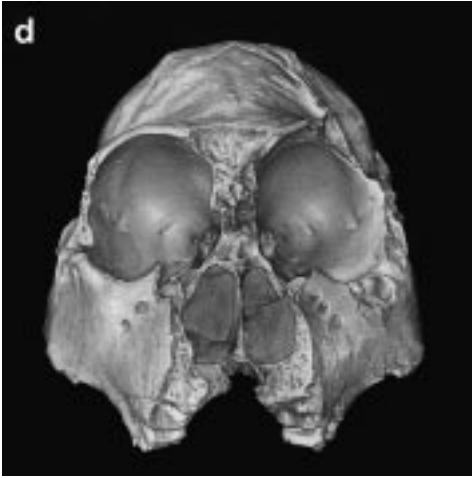


Figure 2. Holotype specimen of *Paralouatta varonai* (MNHNH V194): (a) dorsal, (b) ventral (from a cast), (c) lateral, and (d) frontal views [(a) and (c) from [Rivero & Arredondo, 1991](#)].

passages higher on the mogote through a system of fissures. Evidence for this supposition is the discovery of small bones (not primate) in the upper part of the major vertical fissure which transects Cueva del Mono Fósil, and the fact that all discoveries of consequence made at Cueva Alta came from a single locus—a small, sediment-choked chimney ([Jaímez Salgado et al., 1992](#)). Efforts to date bone from these caves chronometrically have not been successful because the bones retain too little collagen to permit ^{14}C (radiocarbon) dating. Whether this means that they are actually beyond the range of radiocarbon dating has not been established, but it is certainly a possibility. If the Galeras faunule is comparatively old, it would help to explain (although not fully clarify) why monkey bones have not been recovered elsewhere in Cuba.

Craniodental morphology of *Paralouatta*

[Rivero & Arredondo's \(1991\)](#) description of the holotype skull of *P. varonai* focused on systematically important features and was not intended to be comprehensive. In this section we provide a fuller account of this

important fossil, both to round out knowledge of the cranial anatomy of *Paralouatta* and to provide a descriptive basis for some of the character analyses conducted in the next section. It should be noted that the temporary museum number cited by [Rivero & Arredondo \(1991\)](#) for the holotype specimen (MNHNH 90-25) has now been replaced by a permanent accession string (MNHNH V194).

Because the teeth of MNHNH V194 are exceptionally worn, [Rivero & Arredondo \(1991\)](#) were unable to provide an adequate description of the dentition of *P. varonai*. Later collecting has resulted in the discovery of a lower jaw (MNHNH V195) and some 80 isolated teeth, many in excellent condition. These new fossils yield a wealth of detail unknown previously. Our description is conducted by element and we provide measurements of dental elements in [Table 1](#) [for additional measurements, see original description of type skull by [Rivero & Arredondo \(1991\)](#)].

[Rivero & Arredondo \(1991\)](#) interpreted overall skull shape in *Paralouatta* as essentially indicative of alouattine affinity. For example, both display a substantial angle (airorhynch) between the facial and neural regions of the skull. However, *Alouatta* is a

Table 1 Dental measurements (in mm) of new remains of *P. varonai*¹

Specimen	B-L	M-D	
I ¹	V150	3.9	5.9
	V152	3.9	5.7
	V153	4.2	5.4
	V154	3.9	5.6
	V156	3.9	6.1
	V158	4.4	5.8
I ²	V105	3.8	4.3
	V149	4.1	4.7
	V151	3.4	4.2
	V155	3.7	4.1
P ²	V115	5.7	5.5
	V160	5.4	5.3
	V164	4.9	5.3
	V165	6.0	5.4
P ³	V163	7.2	5.1
	V169	8.0	4.9
	V176	8.2	4.6
	V178	7.0	4.5
	V578	8.6	5.3
dP ⁴	V166	6.7	5.6
P ⁴	V106	9.1	5.4
	V116	9.1	5.5
	V170	10.0	5.2
	V171	9.2	5.2
M ^{1,2}	V120	9.1	6.6
	V179	9.0	6.9
	V180	9.7	7.0
	V181	9.3	6.5
	V183	8.8	6.6
M ³	V122	7.0	6.3
	V191	7.2	5.5
	V192	7.1	5.3
I ₁	V126	3.6	2.8
I ₂	V195	3.8	3.2
C ₁	V127	3.2	5.1
	V195	4.1	4.7
P ₂	V117	5.3	5.4
	V128	5.2	5.2
	V195	4.5	4.8
P ₃	V118	5.9	4.9
	V129	5.8	4.9
	V130	5.7	5.4
	V131	5.5	4.7
	V132	5.5	4.9
	V195	5.9	5.9
P ₄	V119	6.7	5.8
	V146	6.6	5.6
	V147	5.8	5.5
	V195	5.9	6.4
M ₁	V195	5.6	7.4
M _{1,2}	V123	5.3	7.1
	V138	5.9	7.0
	V144	6.0	7.1
	V145	5.5	6.6

Table 1 *Continued*

Specimen	B-L	M-D	
M ₂	V195	5.6	7.4
M ₃	V124	5.1	7.8
	V134	4.5	6.6
	V135	5.0	7.0
	V579	5.5	7.8
	V195	5.0	7.2

¹Measurements for best preserved teeth only.

clear outlier among platyrrhines for this feature, while the condition in *Paralouatta* is best described as incipient. Thus, while it can be said that the skulls are broadly similar in this aspect, the two differ in many other characters—as our data matrix brings out. This point applies particularly strongly to the dentition, which was previously poorly known. With the new dental remains of *Paralouatta* now available, it can be shown that the Cuban monkey differs markedly from both *Alouatta* and *Sirtonia*.

Skull

In most respects the neurocranium and basi-cranium of MNHNH V194 are exceptionally well preserved; by contrast, the facial region is damaged extensively (Figure 2).

Frontal. Except for the glabella/nasion region and the orbital processes, the frontal bone is quite complete. Shaped like an isosceles triangle, with its largest dimension oriented anteroposteriorly, the frontal is delimited rostrally by a low supraorbital ridge surmounting the orbits [Figure 2(a)]. Dorsally, each supraorbital ridge is thrown into relief by a slight depression in the frontal, immediately behind the line of the ridge. In lateral view, the typical platyrrhine contact pattern is displayed, with the zygomatic and the parietal interposed between the frontal and alisphenoid. Within the orbit, the frontal runs from dorsolateral to medioventral, intersecting the lateral

orbital fissure. Medial to its contact with the zygomatic, the frontal contacts successively the alisphenoid, the orbitosphenoid (above the orbital foramen) and, slightly more anteriorly on the medial wall of the orbit, the ethmoid (little of which is preserved).

Breakage in the glabellar region provides a window into the midsagittal portion of the frontal sinuses, which appear to have been extensive (see below). Dorsally, the coronal suture is drawn into a long, posteriorly directed "V", corresponding to the two remaining sides of the isosceles triangle. Bregma is located far to the rear, at the transverse level of the posterior carotid foramen (with skull in Frankfurt plane).

Ethmoid. Because of fusions and breakage, sutural boundaries in the ethmoid region cannot be followed for any distance. However, it is clear that the ethmoid was pneumatized extensively and that, in consequence, the interorbital septum was comparatively substantial. The septum's thickness suggests that it was not fenestrated. The anterior portion of the orbital wall and upper face, including the lacrimals and the nasals, are not preserved.

Maxilla. The maxillae are well preserved except for their medial portions. The bony orbits jut from the face to a marked degree (especially evident in *norma verticalis*), which suggests that the eyes were very large, although not as large as in *Aotus* (for observations on orbital size in *Paralouatta*, see [Rivero & Arredondo, 1991](#)). The maxilla extends backward to form much of the orbital floor and the medial side of the inferior orbital fissure (sphenomaxillary fissure) up to the point of contact with the palatine. The facial portions of the maxillae bear multiple infraorbital foramina. The area normally formed by the premaxilla has been lost through breakage, and there are no identifiable remnants of the maxillo-premaxillary suture.

The zygomatic process of the maxilla is situated low on the face. The preserved part of its ventral edge lies just above the plane of the alveolar border (<1.0 times height of M^2 crown), as in *Callicebus* and *Xenothrix* (Horovitz & MacPhee, in prep.). This is in contrast to *Alouatta*, the other atelines, and pitheciins, in which the process's position on the face is notably higher (≥ 1.5 times height of M^2 crown). *Cebus*, *Aotus*, and *Saimiri* display intermediate positions.

The maxillary tuberosity or postdental part of the maxilla is drawn out into a lengthy, triangular process that articulates with the elongated pyramidal process of the palatine [[Figure 2\(b\)](#)]. It is not obvious why the rear of the maxilla should be conspicuously enlarged in *Paralouatta*, as the maxillary sinus does not appear to extend into this region. (However, matrix left within the nasal cavity to provide support for remaining lamellae may obscure an ostium into the tuberosity.) In atelines the tuberosity is quite abbreviated and the posterior wall of the maxilla is much more vertical, especially in *Alouatta*. In contrast, *Cacajao*, *Pithecia*, *Callicebus*, and *Xenothrix* display a somewhat larger tuberosity. Comparisons show that this feature varies conspicuously across platyrrhine genera.

The internal architecture of the nasal cavity is poorly preserved. However, the massiveness of the facial region of the skull, evident in the photographs [[Figure 2\(a\)](#)], is principally due to the expansion of pneumatic spaces related to the nasal apparatus. Both the nasal chamber *per se* and the paranasal sinuses are exceptionally large—indeed, proportionally much larger than in any extant large-bodied platyrrhine. The inferior surface of the nasal aperture is broad and gently sloping. Comparisons reveal some similarities in this respect to *Callicebus* and, to a lesser degree, *Callimico*.

One maxillary turbinal, probably the ventralmost, is partly preserved on the left side. It begins high on the lateral wall of the nasal

cavity, at the level of the highest infraorbital foramen, and is directed medioventrally.

A point of minor paleopathological interest concerns the large abscess chamber perforating the wall of the maxilla above the mesial root of the left M^2 .

Palatine. The palatine bones are partly preserved [Figure 2(b)]. Each maxillo-palatine suture parallels the dental series up to the level of M^2 , then runs medially to meet its fellow (midsagittal contact lost through breakage). The greater palatine foramen, at the level of M^3 , lies on or just medial to the track of this suture.

The posteromedial palatine spine is located posterior to the transverse level of M^3 . Its apparent degree of projection is increased by deep scalloping of the choanal margin of the palatines. The arc of the scallops does not reach the transverse level of M^3 . The palatine enters into the construction of the orbit along the medial wall of the inferior orbital fissure. Posteriorly it contacts the alisphenoid and anteriorly the maxilla.

Vomer. The bladelike vomer is visible on the base of the skull beneath the presphenoid, part of which it covers. Irregularly sutured into the palatines, the vomer extends to the rear edge of the palate and thereby helps to define the choanal apertures. The choanae are relatively enormous (right aperture, 14.1×9.1 mm), their entrances being approximately four times as large in area as those of AMNHM 230805, a specimen of *Alouatta seniculus* of similar skull length (right aperture, 8.6×3.7 mm).

Temporal. The temporal squamae are very low, as in platyrrhines generally, and the postglenoid process is notably elongated. The large postglenoid foramen [Figure 2(b)] is situated on the medial side of the latter process, rather than behind it or within it. There is a pronounced gap between the

anterior crus of the ectotympanic and the postglenoid process; this is unlike most platyrrhines, in which these two structures form a continuous surface or are situated very close together. The squamosal contacts the alisphenoid medially, with which it forms a suture that runs parallel to the midsagittal plane to approximately the level of the lateral pterygoid process. At this point the suture turns laterally and runs along the ventral edge of the parietal.

The ectotympanic is completely fused to the tympanic bulla (here assumed to be petrosal in origin); no sign of a suture remains. The aperture of the meatus is an oval ring, the long axis of which runs anteroventrally/posterocaudally. The meatal margin is raised and highly rugose except on its dorso-caudal face, which is smooth and flattened.

The elongated tympanic bullae are moderately inflated. The anteromedial portions of both are broken, thus exposing parts of the middle ear cavity. As seen from the outside, the alisphenoid forms the rostral and lateral edges of the foramen ovale, while the bulla makes up this aperture's medial and caudal edges. The canal for the auditory tube opens immediately beneath the caudal border of the foramen ovale. The posterior carotid foramen is located on the medial curvature of the bulla in the typical platyrrhine position, just in advance of a line connecting the jugular foramina. It is recessed into a small basin whose border is defined by a sharp line or crest on the bulla's ventral surface. The stylomastoid foramen, which is only slightly smaller than the carotid foramen, is located posteriorly on or near the apparent margin of the ectotympanic. The hypoglossal canal is buried in a deep pit above the anterior margin of the occipital condyles.

The petrosal promontorium, seen by looking through the external auditory meatus, displays two bulges or prominences. The first is the margin of the aperture of

the fenestra cochleae; the second bulge, situated more anterodorsally, appears to be either a bony eminence or (more likely) the next turn of the cochlea itself, seen in relief as it swells the lateral aspect of the promontorium. Similar bulges are present in *Callicebus*, *Pithecia*, callitrichines, *Cebus*, *Saimiri*, and *Aotus*. In all other genera examined by us the promontorium is either without relief in this region or only the first bulge is present.

Paralouatta has a typically anthropoid anterior accessory (paratympanic) cavity whose posterior wall is partly defined by the track of the bony carotid canal (see MacPhee & Cartmill, 1986). The dorsally placed epitympanic recess is large and filled with short, irregular septa. Similar relief is also present in the posterior part of the hypotympanic region.

The posterior end of the temporal is completed by the mastoid region. In *Paralouatta* the mastoids are considerably swollen, and they project laterally and especially posteriorly much more than in *Alouatta*. Small fenestrations created by breakage expose bony cellules within the mastoids, indicating significant pneumatization.

Sphenoid complex. The ventral aspect of the sphenoid complex is unremarkable. The presphenoid–basisphenoid synchondrosis is completely fused, although a faint line marks its original position. Cellules of large size (possibly evidence of pneumatization) have been exposed by abrasion at the site of the basisphenoid–basioccipital synchondrosis. The body of the basisphenoid bears low ridges paralleling the tympanic bullae, probably for the origin of prevertebral muscles (see description of occipital).

The dorsal wing of the alisphenoid contacts the zygomatic, parietal, and squamosal. The dorsal wing forms the lateral edge of the inferior orbital fissure. The ventral (pterygoid) wing forms a small fraction of the medial edge of the inferior orbital fissure

and most of the pterygoid process (the anterior third of each process is contributed by the palatine). Neither the lateral nor the medial pterygoid plates are completely preserved, but it is clear that the lateral plates were much larger than the medial, as in platyrrhines generally. It is not possible to determine whether the medial plates projected substantially. However it is possible to see that the pterygoid fossa between the medial and lateral pterygoid processes was very shallow and did not excavate the base of the skull. In this regard *Paralouatta* is similar to *Callicebus*, pitheciins and atelines, but contrasts markedly with *Cebus*, *Saimiri*, and *Aotus*, in which the fossa indents the skull base.

Parietal. In *Paralouatta* the parietals meet the zygomatics along an irregular, dorsoventrally oriented line. A projecting portion of the parietal's ventralmost edge intervenes between the zygomatic and the alisphenoid, and thereby manages to border on the lateral orbital fissure. Parietal contribution to the delimitation of the lateral orbital fissure is a character present (although frequently polymorphic) in most platyrrhines. However, in *Alouatta*, *Brachyteles*, and *Cebus*, the lateral orbital fissure is normally defined by the zygomatic exclusively, or by this bone and (for a small distance) the alisphenoid. The parieto–alisphenoid suture, about one-quarter of the length of the parieto–squamosal contact, terminates close to the posterior (squamosal) root of the zygomatic arch.

As seen from above, the temporal lines are remarkably sinusoidal, flaring once anteriorly (at the level of the supraorbital ridge), again centrally (at bregma), and once again posteriorly (just in advance of the lambdoidal suture).

Zygomatic. This bone is not preserved completely on either side: the orbital margins are missing bilaterally, and the zygomatic

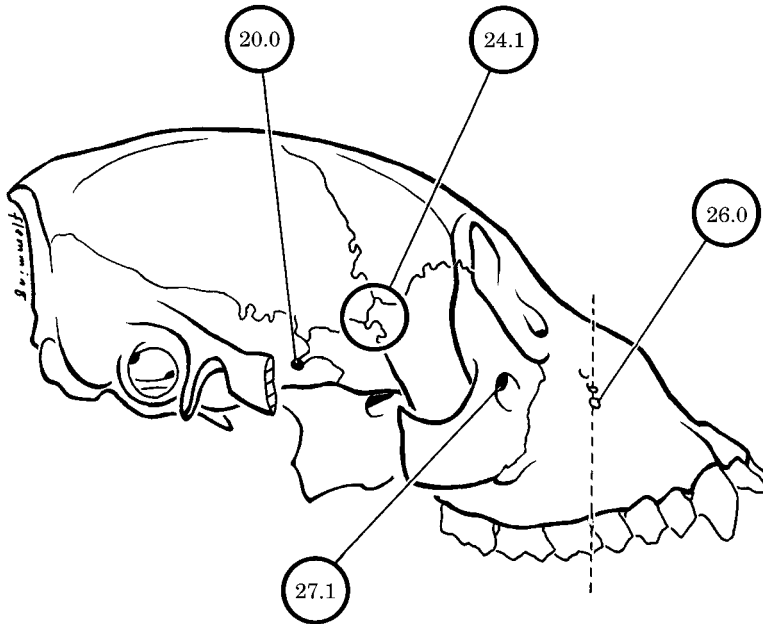


Figure 3. Skull of adult *Alouatta* (lateral view) showing several characters (see Appendix 1).

roots of the zygomatic arches are only partially preserved. The fronto– and parieto–zygomatic sutures and the formation of the lateral orbital fissure have already been described. The maxillo–zygomatic suture slants posteroventrally, with the result that the maxilla and the zygomatic form respectively the ventral and dorsal halves of the root of the zygomatic arch.

Multiple zygomaticofacial foramina are located on the face, near the ventrolateral margin of each orbit (although this is not obvious in the figures because of breakage). At least three foramina are preserved on the right side, the central one being the largest [see Rivero & Arredondo (1991)]. In most platyrrhines, there is a single zygomaticofacial foramen on each zygomatic (Figure 3); however *Alouatta*, some pitheciins, and *Aotus* occasionally display multiple foramina.

Occipital. The basioccipital widens caudally. Its ventral surface is marked by the continuation of the low ridges for muscle attachment seen on the basisphenoid.

Ridging is extensive, more so than in any living platyrrhine, including *Alouatta*. The width of the skull in norma occipitalis is considerably increased by the lateral projection of the mastoids.

The skull qualifies as airoryhynchic because the basioccipital is angled (ventrally flexed) with respect to the dental series, somewhat more than most platyrrhines except *Alouatta*, in which the angle is markedly larger.

The foramen magnum is positioned so that it faces downward as much as backward when the skull is placed in the Frankfurt plane, as in platyrrhines other than *Alouatta*. By contrast, in *Alouatta* the foramen magnum is more posteriorly positioned and is oriented at a sharp angle to the basioccipital.

The supraoccipitals form an angle of approximately 45° with the Frankfurt plane. The surface of the occipital planum is exceptionally rugose, suggesting that there was a considerable investment in postural muscle mass.

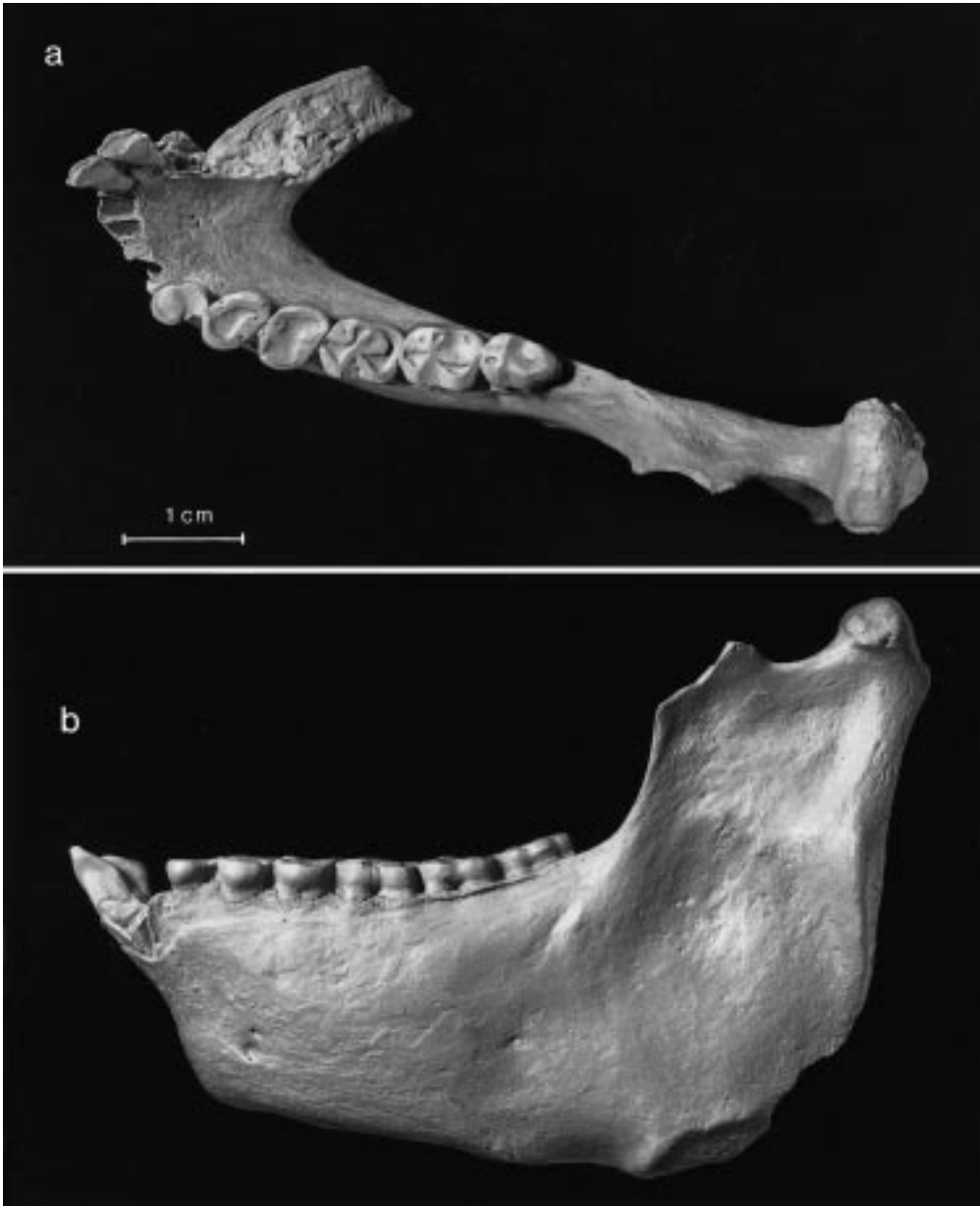


Figure 4. *Paralouatta varonai* mandible (MNHNH V195), in (a) occlusal and (b) lateral views.

Mandible

The mandible (MNHNH V195) of *Paralouatta* was found in 1991 in Cueva del Mono Fósil, but at a considerable remove from the position of discovery of the type skull. The mandible (Figure 4) is that of an

adult animal, although it is far too small to articulate with the type skull. The specimen preserves the left ascending and horizontal rami, with P_2 – M_3 *in situ* and alveoli for other anterior teeth, the symphyseal portion, bearing I_2 and C_1 and a small part of the inferior

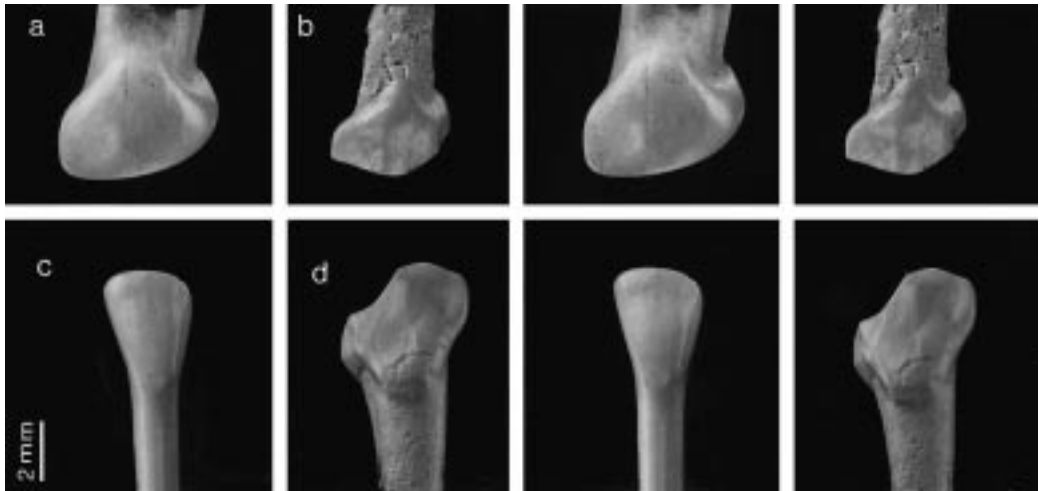


Figure 5. *P. varonai*, stereoscopic views of isolated front teeth: (a) I¹ (MNHNH V154), (b) I² (MNHNH V155), (c) I₁ (MNHNH V126), and (d) C₁ (MNHNH V127).

border of the right horizontal ramus. On the preserved left ascending ramus, the coronoid process is broken at its root and the medial aspect of the mandibular condyle is abraded. Otherwise, the specimen is in extremely good condition. However, as the teeth of both the type skull and the mandible are exceedingly worn, descriptions of individual loci are based largely on isolated specimens found during screening operations at Cueva Alta.

Dentition

Although [Rivero & Arrendondo \(1991\)](#) concluded that *P. varonai* was a definite alouattin, they noted that the teeth of the Cuban species appeared to differ in several ways from those of howler monkeys. Thus they noted that molar pericones were present and large, and that, curiously, the maxillary canine (as indicated by a preserved root) would have been tiny. Additional marked differences between *Paralouatta* and *Alouatta* were briefly documented by [MacPhee et al. \(1995\)](#).

To a greater degree than in any other known platyrrhine, the entire dental series of *Paralouatta* evidently wore down in such a

way that asperities (cusps and cristae) were rapidly removed, effectively converting the occlusal surfaces of the cheek teeth into large, flat milling surfaces (see [Figure 4](#)). *Paralouatta* is unusual in displaying, in combination, the following features usually associated with hominine dentitions: extreme bunodonty, premolar hypertrophy, widened maxillary incisor crowns, and, most interestingly, marked canine reduction (crowns incisiform, projecting little or not at all beyond occlusal plane of cheek teeth, and canine root small).

The dental formula of *Paralouatta* is 2133/2133, as in all known platyrrhines except callitrichines (other than *Callimico*) and *Xenothrix*.

Maxillary teeth

Central incisors. MNHNH V150, 152–154, 156–158. Large size (compared to lateral incisors), substantial breadth, and low crown height are noteworthy features of the maxillary central incisors [[Figure 5\(a\)](#)]. In *Alouatta*, *Brachyteles*, *Ateles*, and, to a lesser degree, *Lagothrix*, incisors are higher-crowned but narrower. As is frequently the case in platyrrhines, the mesial margin of

the crown is higher than the distal, and the biting edge is distinctly curved. On little-worn specimens, a bean-shaped fovea is visible on the lingual surface.

Incisor tooth use in *Paralouatta* seems to have involved considerable amounts of bite-pulling, because worn teeth display numerous small grooves arrayed normal to the edge of the occlusal surface. Wear features suggest that maxillary incisors were drawn orthally across lowers during biting, or that food items were shredded by pulling them manually between clenched incisor teeth. As a result, wear on the lingual or foveal surface of I^1 is often substantial (for example, all enamel lost from foveal surface MNHNH V158). Step-fracturing and pitting of the enamel is visible in, and restricted to, the areas immediately adjacent to the bite surface. This localization suggests that these defects were acquired during life, probably as the result of small fragments of enamel spalling off during powerful biting.

Lateral incisors. MNHNH V105, 149, 151, 155. Maxillary lateral incisors have shorter roots, considerably smaller crowns, and narrower cervical regions than do central incisors [Figure 5(b)].

Characteristic of I^2 s of *Paralouatta* is the presence of interproximal facets on both the mesial and distal margins of the crown. The existence of the distal interproximal facet implies that I^2 and C^1 were in permanent contact, that is, they were not separated by a diastema. (This point was not obvious when only the type skull was available, since it lacks incisors and preserves only the stump of one canine root.) In this feature *Paralouatta* is unlike any living large-bodied New World monkey, in all of which the canines are enlarged and diastemata are present. In these latter platyrrhines, the distal aspects of I^2 crowns sometimes display an oval facet for the mesial aspect of the tip of C_1 . However, because the C_1 meets the I^2 at an oblique angle, the resulting facet is never vertically

aligned. In *Paralouatta*, the I^2 distal facet is vertical, circular rather than oval in form, and separated from faceting on the bite edge by a significant gap. Therefore it cannot be a C_1 facet, but must instead be for the C^1 . Taken together, these features strongly imply that in the Cuban monkey, maxillary incisors and canines were in intimate contact and prone to develop interproximal faceting.

Canine. MNHNH V194. The type skull retains only the deepest part of the root of the right C^1 , which at that level, is smaller than the alveolus for P^2 . The tiny size of this root was confirmed by X-ray of the holotype.

Premolars. MNHNH V115, 160–162, 164, 165 (P^2); 163, 169, 174–178, 578 (P^3); MNHNH V106, 116, 167, 168, 170–173 (P^4); MNHNH V166 (dP^4).

P^2 (MNHNH V115, 165) is double-rooted in the type specimen (MNHNH V194), as reported by Rivero & Arredondo (1991). However, the three isolated specimens in which the roots are complete or nearly complete (V160, 162, 164, 165) are in fact single-rooted, as is normally but not universally the case in other platyrrhines (Hershkovitz, 1977). For example, in most specimens of *Callicebus* the P^2 root is single and undivided, but a split root is occasionally seen. P^2 bears a single cusp on its buccal side, and its trigon widens distally [Figure 6(a)]. P^3 and P^4 [Figure 6(b), (j)] are morphologically similar, although P^3 is somewhat smaller. Both of the distal premolar loci bear two cusps, with the protocone being situated in the mesiobuccal quarter of the trigon. The lingual cingulum is prominent and mesially projecting relative to the trigon (cingular buccolingual width at least half that of trigon). In the type specimen, both P^3 and P^4 exhibit two buccal roots in addition to a lingual root. Among isolated specimens, MNHNH V163 and V178 (both P^3 s) are single-rooted, whereas MNHNH

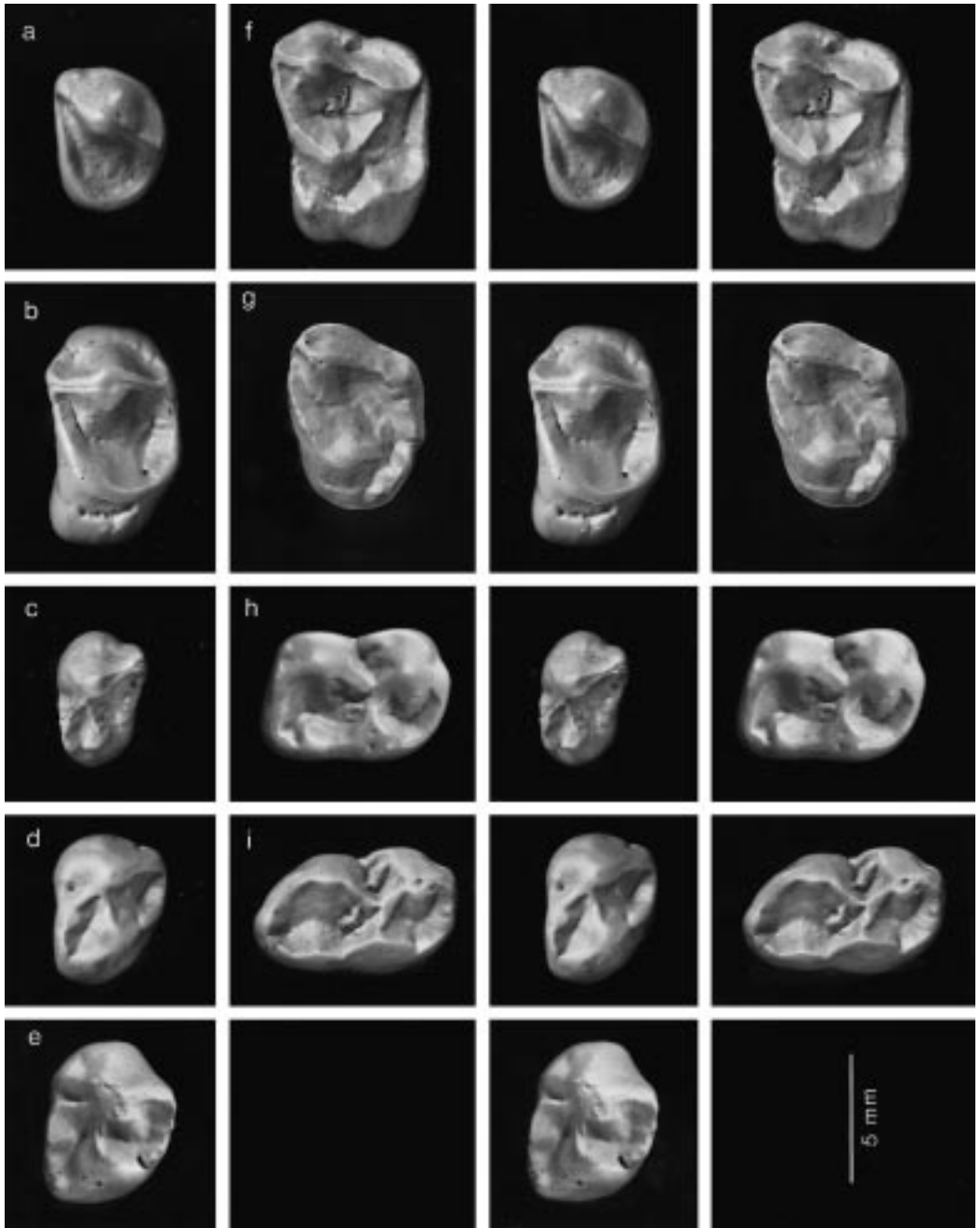


Figure 6.

V106 (a P⁴) has two roots (one buccal, one lingual). Platyrrhines display some variability in root number in P³ and P⁴. In *Cebus*,

Saimiri, *Aotus*, *Cacajao*, *Alouatta*, *Callicebus*, and *Xenothrix*, P³ normally possesses two roots (three occasionally in *Alouatta*). On

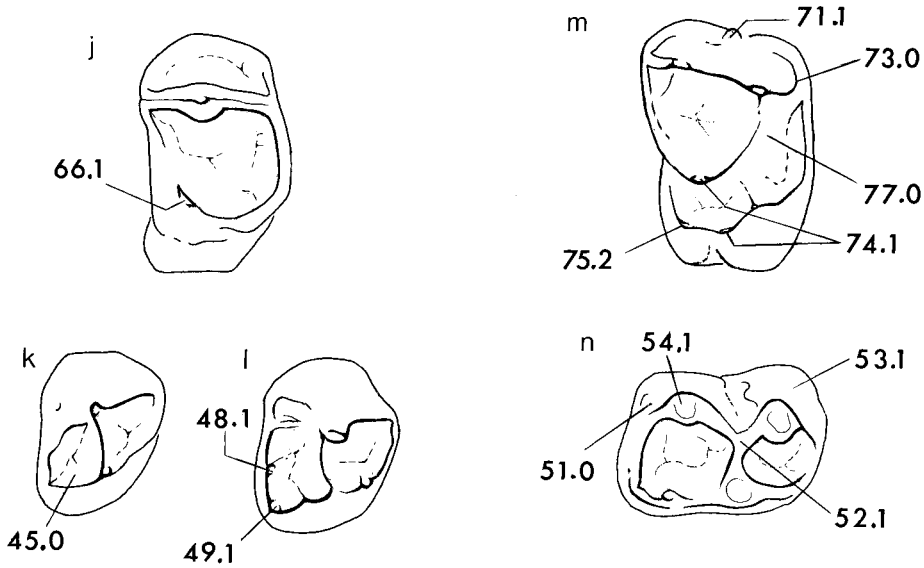


Figure 6. *P. varonai*, stereoscopic views of permanent premolars and molars with explanatory keys: (a) P² (MNHNH V115), (b) P⁴ (V116), (c) P₂ (MNHNH V117), (d) P₃ (MNHNH V118), (e) P₄ (MNHNH V119), (f) M^{1,2} (MNHNH V120), (g) M³ (MNHNH V122), (h) M_{1,2} (MNHNH V123), (i) M₃ (MNHNH V124), (j) P² (MNHNH V115), (k) P₃ (MNHNH V118), (l) P₄ (MNHNH V119), (m) M^{1,2} (MNHNH V120), and (n) M_{1,2} (MNHNH V123).

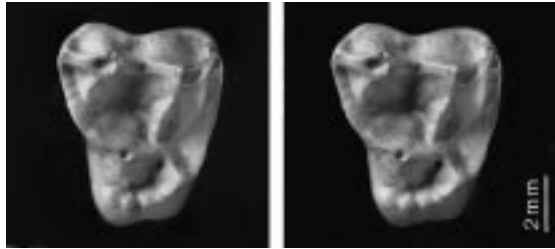


Figure 7. Stereoscopic view of *P. varonai* deciduous P⁴ (MNHNH V166).

the other hand, in *Ateles* the roots of P³ tend to be fused and only the tips of the roots are separate. P⁴ normally has two roots in *Cebus*, *Saimiri*, *Cacajao*, *Alouatta*, *Callicebus*, and *Ateles* (as in P³, tips barely separate); in *Aotus* the normal condition is three roots.

Only one deciduous premolar, a dP⁴ (MNHNH V166), has been recognized with certainty (Figure 7). Very low crowned with three broadly splayed roots (two buccal, one lingual), it resembles upper molars in general outline, but the proportions of the major cusps are somewhat different. The lingual

cingulum is less developed (crown more triangular), and overall the tooth is much smaller than true molars.

Molars. MNHNH V104, 120, 121, 179–184, 186–190 (M^{1,2}); MNHNH V122, 185, 191–193 (M³). We have found no reliable way to separate first and second upper molars, and therefore will discuss them together.

Upper molars of *Paralouatta* display several diagnostically interesting features. One such feature is the size and differentiation of cingular structures [Figure 6(f), (m)].

Except on the mesial side of molar trigons, a continuous ledge borders upper molar crowns; the ledge is best developed buccally and lingually. In the least worn examples of $M^{1,2}$ (e.g., MNHNNH V120, 180), the buccal cingulum is continuous from the preparacrista to the postmetacrista, although it is scored by a tiny groove in the ectoflexus. The buccal cingulum is adorned with a relatively discrete distostyle distobuccally, a very faint parastyle, and two low bumps (=mesostyles) on either side of the groove in the ectoflexus.

The lingual cingulum is massively developed and forms a continuous band from the mesiolingual aspect of the protocone to the distostyle of the buccal cingulum. There is a well-developed hypocone and a smaller but nevertheless well-developed entostyle (=pericone), doubled in some specimens (e.g., MNHNNH V120, 180). The hypocone is connected to the metaloph via a well-developed prehypocrista (hypocone crest). The hypocone is large in howler monkeys, and there is a deep incisure between the hypocone and protocone that is lacking in *Paralouatta*.

One of the outstanding features of molar construction in *Paralouatta* is the position of the protocone, which appears to be situated virtually in the centre of the occlusal surface. This appearance is in large measure due to the great width of the lingual cingulum, which isolates the protocone from the crown margin. In *Alouatta*, the protocone is not lingually bordered by a cingulum at all, while in *Stirtonia* (see Material and methods) the latter is very narrow and discontinuous.

The major trigon cusps are markedly bunodont and enclose a large but shallow trigon basin. In unworn teeth (MNHNNH V120, 180), the deepest part of the basin is corrugated by a number of tiny cuspules and grooves. However, the type of crenulation is not readily comparable to that seen on pitheciin molars; in the latter they are much finer, and have the shape of elongated

ridges. As in other platyrrhines, $M^{1,2}$ display three roots, two buccal and one lingual.

M^3 , smaller than $M^{1,2}$, displays four cusps, of which the paracone is best developed. The hypocone appears on the lingual cingulum bordering the distal side of the tooth and is barely cuspidiform. The floor of the trigon is irregularly rugose, as in $M^{1,2}$. This tooth may exhibit two discrete roots (as in MNHNNH V185, 193) or only a single, fused one (MNHNNH V122, 191, 192) [Figure 6(g)].

Mandibular teeth

Central and lateral incisors. MNHNNH V126 (I_1); MNHNNH V195 (I_2). The narrow-crowned I_1 and I_2 are tiny compared to the upper incisors [Figure 4, 5(c)]. There is only one identifiable I_1 in the existing sample (MNHNNH V126); its flat occlusal edge presents a large dentine lake exposed through wear. Central incisors are missing in the jaw (MNHNNH V195), but I_2 is preserved on the right ramus. Compared to I^1 , the I_1 has a narrower crown and a smaller root (as suggested by empty alveoli in the jaw). In both teeth, many sub-parallel striations can be seen running normal to the bite surface (cf. maxillary incisors).

Canine. MNHNNH V195, 127 [Figure 4, 5(d)]. The C_1 is present *in situ* in the Mono Fósil lower jaw (MNHNNH V127); this specimen demonstrates beyond any doubt that extreme canine reduction was the normal condition in *Paralouatta*. It is also clear from this specimen that C_1 was no more projecting than P_2 , from which it may be distinguished only by its greater degree of buccolingual compression and single, blade-like, mesiodistally oriented principal cusp. A subtle lingual cingulum is present in V127.

Premolars. MNHNNH V195 (mandible with P_{2-4}); MNHNNH V117, 128 (P_2); MNHNNH V118, 129–132 (P_3); MNHNNH V119, 146–148 (P_4). Dimensions of mandibular

premolars increase distally, making P_2 the smallest member of the premolar row (Figure 4). This premolar locus–size relationship is seen in other platyrrhines having diminutive canines (e.g., *Callicebus*). In contrast, in all atelines except *Brachyteles*, P_2 is the largest premolar. In *Paralouatta*, P_2 and P_3 are single-rooted; none of the isolated P_4 s has a completely preserved root.

The P_2 has one buccal cusp from which radiate three crests: one runs mesially, another curves slightly as it passes distolingually, while the third and shortest crest originates slightly distal to the cusp, runs lingually, and ends in a small swelling [Figure 6(c)]. About twice as much of the tooth is located mesial to the last crest as lies distal to it. The cingulum is not continuous around the lingual and distal surfaces of the P_2 crown (as it is in atelines) because it is interrupted by the lingual crest.

The P_3 has two distinct cusps of subequal height, a metaconid and a larger (in diameter) protoconid. A crest running mesially from the metaconid describes a sharp angle and then curves distolingually onto the protoconid. The talonid bears no cusps, is longer mesiodistally on the lingual side, and is completely enclosed by a crest. The trigonid is notably larger than the talonid [Figure 6(d), (k)].

The P_4 , the largest of the three premolars [Figure 6(e), (l)], has a square outline and a well developed protoconid and metaconid. Both cusps are subequal in height, but the protoconid has a much larger volume than the metaconid. As in the molars, the buccal (protoconid) side of the tooth is swollen and projecting. Trigonid and talonid basins are originally distinct, but quickly become worn down to shallow grooves. It displays hypoconid and entoconid.

Molars. MNHNH V195 (mandible with M_{1-3}); MNHNH V123, 136, 138–142, 144, 145, 579 ($M_{1,2}$); MNHN V124, 134, 135 (M_3).

As in the case of M^1 and M^2 we cannot identify any consistent morphological or size differences between M_1 and M_2 . All mandibular molars display two roots, one mesial and the other distal.

Compared to *Alouatta*, lower molar cusps are stouter, crests are much less marked even in unworn teeth, and in worn teeth there is almost no difference in cusp height profile between talonid and trigonid cusps [Figure 6(h), (n)].

Alouatta and *Stirtonia* distinctively differ from *Lagothrix*, *Ateles*, and *Brachyteles* in that the talonid is transversely wider than the trigonid. Inspection shows that breadth difference is mainly due to the fact that, in *Alouatta*, the apex of the entoconid bulges lingually to a noticeable degree, giving the talonid an almost pear-shaped outline. *Paralouatta* critically differs in that protoconid and hypoconid apices are not displaced. Instead, the entire buccal aspect of the lower molars is swollen, making the protoconid and hypoconid seem proportionately larger than the metaconid and entoconid and giving the tooth a lop-sided look, similar to *Xenothrix* molars (see figure in Williams & Koopman, 1952).

The distal wall of lower molar trigonids is a continuous, raised crest joining metaconid and protoconid. It is on a sharp oblique, as in *Alouatta* and *Stirtonia*. In all molars the cristid obliqua (=premetacristid) is strongly built and intersects the distal wall of the trigonid at a position intermediate between the protoconid and metaconid. As a result the ectoflexid is very deep in all lower molars, its apex being situated within the middle one-third of the tooth's breadth. In little-worn specimens (e.g., V579) the ectoflexid is frequently adorned with one or two small cuspules (ectostylids), usually positioned on the distobuccal wall of the protoconid.

On M_3 there is a hypoconulid, of moderate size, situated directly distal to the entoconid and separated from it by a sulcus leading into a small distolingual basin [Figure 6(i)].

The hypoconulid is occasionally present on the M_3 of many platyrrhine species.

Cladistic analysis

Materials and methods

A total of 80 characters are listed and defined in Appendix 1. These are scored in Appendix 2 for the taxa making up the comparative set, which include *Cebupithecia*, *Stirtonia*, *Paralouatta*, *Antillothrix*, *Xenothrix*, the 16 extant genera of New World monkeys, and several outgroups. *Cebupithecia sarmientoi* (Stirton & Savage, 1951), *Stirtonia tatacoensis* (Stirton, 1951; Herschkovitz, 1970) and *S. victoriae* (Kay *et al.*, 1987) are fossil species from the Middle Miocene of Colombia. *C. sarmientoi* has been previously placed among pitheciines (Stirton & Savage, 1951; Stirton, 1951; Orlosky, 1973; Rosenberger, 1979; Kay 1990). *Stirtonia* is currently considered the sister group of *Alouatta* (Rosenberger, 1979; Setoguchi *et al.*, 1981; Kay *et al.*, 1987, 1989). As mentioned in the Introduction, *P. varonai*, *A. bernensis*, and *X. mcgregori* are Quaternary species from Cuba, Hispaniola and Jamaica respectively. Character analysis of *X. mcgregori* is based on the type mandible plus several new fossils recently collected by RDEM, Donald A. McFarlane (CMC), and co-workers in southern Jamaica (two partial mandibles, a maxillary fragment, and a partial skull preserving the palate and most of the nasal fossae and maxillary sinuses; Horovitz *et al.*, 1997). Outgroup taxa consisted of *Tarsius*, a wide array of living catarrhines (including both cercopithecoids and hominoids), and the Oligocene Fayum anthropoid *Aegyptopithecus*. Unlike most fossil taxa that might have been used as outgroups in this investigation, *Aegyptopithecus* is represented by relatively complete skeletal remains and could therefore be scored for many characters.

Most of the characters utilized in this study are based on craniodental mor-

phology, although a few pertain to the postcranium and soft tissue anatomy. Characters taken from the literature were verified before utilization. With respect to continuous characters, we used only those that showed states separated by gaps in distribution among groups of terminal taxa. These characters were considered additive. Missing characters were scored as question marks (see Appendix 2). Phylogenetic analysis was performed using the program *PAUP* (Phylogenetic Analysis Using Parsimony), version 3.1.1 (Swofford, 1993) applying a heuristic search with stepwise random addition sequence of taxa and TBR, done over 100 replications. All characters were weighted equally and variable ones were considered polymorphic. Trees were rooted by designating *Tarsius* as the outgroup.

We obtained Bremer support values for each branch (Bremer, 1988; Källersjö *et al.*, 1992), inspecting the strict consensus of trees up to four steps longer than the most parsimonious ones. For example, branches that collapse in a strict consensus of trees a step longer than the minimum, have a Bremer support of "1".

Results

The heuristic search yielded three most parsimonious trees (CI=0.51, RI=0.66, tree length=269 steps) the strict consensus of which is shown in Figure 8. In this consensus, *Aegyptopithecus* is positioned as the sister group of all other anthropoids, and platyrrhines appear as monophyletic. The three trees differ in how relationships among atelines are portrayed. *Brachyteles* appears either as the sister group of the *Alouatta*–*Stirtonia* dyad (with *Lagothrix*–*Ateles* as the next branch), or as basal within atelines. In the latter case, *Ateles* appears either as the next offshoot within atelines, or as the sister group of *Lagothrix*. Characters supporting all clades in the trees represented by the consensus depicted in Figure 8 are listed in Table 2.

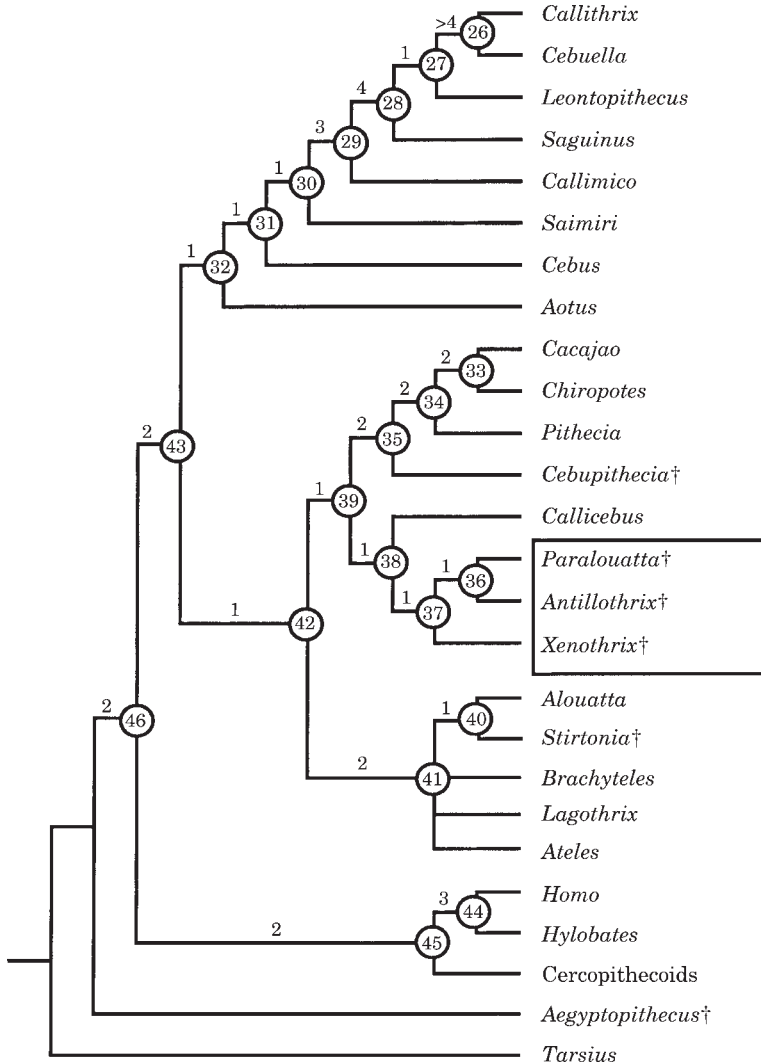


Figure 8. Strict consensus of the three most parsimonious trees obtained with 80 morphological characters (see Appendices 1 and 2); “†” indicates fossil taxon. Antillean clade enclosed in rectangle. Unambiguous character support for each node (labelled with circles) shown in Table 2. Numbers above branches indicate level of Bremer support.

The Bremer support values (Figure 8) indicate that most branches of the depicted topology are unstable, including the relationships of *Paralouatta* to the other Antillean monkeys and *Callicebus*. The topology suggested by the original description of *Paralouatta* (Rivero & Arredondo, 1991), in which *Paralouatta* is regarded as the sister group of *Alouatta*, is 11 steps

longer than the most parsimonious tree. A slightly different formulation, ten steps longer than the most parsimonious tree, has *Paralouatta* as sister group of the *Alouatta*–*Stirtonia* pair. Though our new hypothesis may be falsified with new data, it contradicts rather strongly the contention that *Paralouatta* may be closely related to *Alouatta*.

Table 2 Unambiguous characters supporting tree nodes depicted in **Figure 8**¹

Branch	Character	Change	
node_47→node_46	47. P ₄ metaconid/protoconid height	0→1	
	48. P ₄ hypoconid presence/absence	0→1	
	49. P ₄ entoconid presence/absence	0→1	
	55. M _{1,2} buccal cingulum presence/absence	1→0	
	73. M ¹ postmetacrista slope	0→1	
node_46→node_43	13. Tentorium cerebelli ossification	0→1	
	17. Canal subarcuate fossa/sigmoid sinus	0→1	
	24. Pterion region contact	1→0	
	78. M ³ /P ⁴ length	3→2	
node_43→node_32	15. Paired prominences in middle ear	0→1	
	46. P ₃ meta/protoconid height	1→2	
	54. M ₁ entoconid position	1→0	
	58. M ₃ /P ₄ length	3→2	
	60. I ¹ lingual heel presence/absence	1→0	
node_32→node_31	78. M ³ /P ⁴ length	2→1	
	58. M ₃ /P ₄ length	2→1	
node_31→node_30	38. C ₁ lingual cingulum spike-like vertex	0→1	
node_30→node_29	40. dP ₂ angle mesiodistal axis/postprotocristid	1→0	
	79. M's parastyles presence/absence	0→1	
	6. Presence of claws	0→1	
	21. Eyeball physically enclosed	0→1	
node_29→node_28	22. Cranial capacity	1→0	
	48. P ₄ hypoconid presence/absence	1→0	
	49. P ₄ entoconid presence/absence	1→0	
	1. Number of offspring at a time	0→1	
	16. Pterygoid fossa depth	0→1	
	44. P ₃ /P ₄ protoconid size	0→1	
node_28→node_27	58. M ₃ /P ₄ length	1→0	
	72. M ¹ hypocone/prehypocrista presence/absence	1→2	
	76. M ² hypocone presence	1→0	
	78. M ³ /P ⁴ length	1→0	
	14. Pneumatization in middle ear	0→1	
node_27→node_26	28. dI ₂ shape	1→0	
node_26→node_25	29. I ₁ /I ₂ height	2→1	
	30. I ₁ /I ₂ alignment	0→1	
	31. I _{1,2} shape	0→1	
	32. Meso- and distostyles of I _{1,2}	0→1	
	34. C ₁ root shape	0→1	
	35. C ₁ lingual cingulum	1→0	
	38. C ₁ lingual cingulum spike-like vertex	1→0	
	45. P ₃ /P ₂ talonid	0→1	
	47. P ₄ meta/protoconid height	1→0	
	63. dP ² trigon	1→0	
	node_43→node_42	16. Pterygoid fossa depth	0→1
		41. dP ₂ cross section shape	1→0
	node_42→node_39	56. M ₂ trigonid/talonid height	0→1
	node_39→node_35	72. M ¹ hypocone/prehypocrista presence/absence	1→0
33. Diastema between C ₁ and I ₂		0→1	
36. C ₁ lingual crest sharpness		0→1	
37. C ₁ lingual cingulum mesial elevation		1→0	
58. M ₃ /P ₄ length		3→2	
61. I ² orientation		0→1	
65. P ³ preparacrista		0→1	
59. Molar enamel surface		0→1	
node_35→node_34	67. P ⁴ lingual cingulum	1→0	

Table 2 *Continued*

Branch	Character	Change
node_34→node_33	70. P ⁴ /M ¹ buccolingual breadth	0→1
	72. M ¹ hypocone/prehypocrista presence/absence	0→1
node_39→node_38	15. Paired prominences in middle ear	0→1
	23. Zygomatic arch ventral extent	1→0
	34. C ₁ root shape	0→1
	62. C ¹ /P ⁴ alveolus size	0→1
node_38→node_37	25. Nasal fossa width	0→1
	39. C ₁ /P ₄ buccolingual alveolus size	0→1
	53. M ₁ buccal bulging of protoconid	0→1
node_37→node_36	52. M ₁ oblique cristid and protolophid intersection	0→1
	68. P ⁴ lingual cingulum mesial projection	0→1
	70. P ⁴ /M ¹ buccolingual breadth	0→1
	75. M ¹ pericone/lingual cingulum presence/absence	1→2
	73. M ¹ postmetacrista slope	1→0
node_42→node_41	74. M ¹ protocone/hypocone alignment	0→1
	2. Number of lumbar vertebrae	0→1
	5. Ventral glabrous surface on tail presence/absence	0→1
	20. Temporal emissary foramen presence/absence	1→0
	66. P ⁴ protocone position	1→0
	67. P ⁴ lingual cingulum	1→0
node_41→node_40	52. M ₁ oblique cristid and protolophid intersection	0→1
node_46→node_45	7. Carpo-metacarpal joint of thumb	0→1
	19. Ectotympanic shape	1→0
	67. P ⁴ lingual cingulum	1→0
node_45→node_44	4. External tail, presence/absence	1→0
	8. Rib cage shape	0→1
	9. Ulnar participation in wrist	0→1
	10. Sternebral proportions	0→1

¹Based on morphological data set shown in Appendices 1 and 2.

Three unique, unambiguously positioned characters support Platyrrhini: presence of an ossified tentorium cerebelli (Character 13), presence of a canal which traverses the posterior wall of the subarcuate fossa to connect with the channel for the sigmoid sinus (Character 17), and zygomaticoparietal contact (Character 24). These characters constitute a morphology-based argument for platyrrhine monophyly and deserve additional comment.

Character 13. Hershkovitz (1977) noted that the tentorium is extensively ossified in atelines and, to a lesser degree, in other platyrrhines; tentorial ossification also occurs in lemuroids. However, we find that, as a group, platyrrhines may be distin-

guished from other primates by the fact that tentorial ossification extends behind the subarcuate fossa as well as above and in front of it (Figure 9). Nevertheless, New World monkeys differ in the degree to which the tentorium is ossified. In atelines ossification is always extensive, whereas in some callitrichines and some specimens of *Saimiri* only the portion of the tentorium attaching to the petrosal apex displays any sign of bone formation. Indeed, in some specimens of *Saimiri* there is no indication of tentorial ossification at all, and for this reason we score this character as polymorphic in squirrel monkeys (see Appendix 1).

Our survey of other primates showed that lemuroids characteristically present a restricted, T-shaped tentorial ossification in

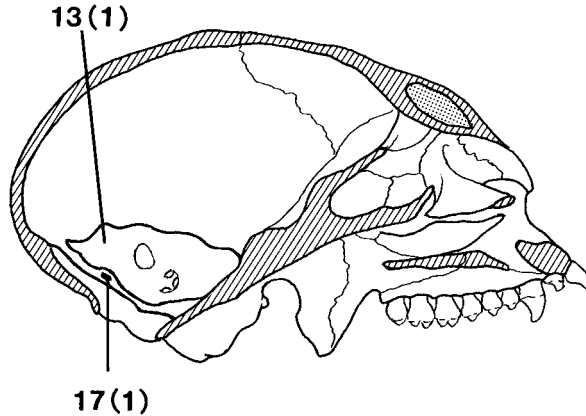


Figure 9. Medial view of sagittal section of *Callicebus moloch* skull (after Hershkovitz, 1977), illustrating partial ossification of tentorium cerebelli (Character 13) and presence of canal connecting subarcuate fossa and sigmoid sinus (Character 17).

front of the petrosal apex, quite unlike the platyrrhine condition. Like catarrhines and *Tarsius*, lemurs lack a posterior extension of tentorial ossification behind the subarcuate fossa. The presence and nature of tentorial ossification could not be determined in our sample of fossil Old World anthropoids.

Character 17. The innominate canal connecting the subarcuate fossa and sigmoid sinus was first identified by Cartmill *et al.* (1981). This canal is located behind and below the aperture of the vestibular aqueduct, and is presumably for venous drainage. Although Cartmill *et al.* (1981) reported this canal to be absent in atelines, we determined on the basis of our more extensive sampling that this feature is regularly present in all New World monkeys, including atelines (feature not yet confirmed for poorly-sampled *Brachyteles*). The vessel traversing the canal does not appear to be the homolog of the sigmoido-antral vein and canal described by Saban (1963) in lemurines in approximately the same location. In lemurines this vein issues from the mastoid antrum and drains to the sigmoid sinus, but in platyrrhines there is no evidence of a mastoid connection.

Two anthropoid petrosals from the Fayum Oligocene were described by Cartmill *et al.* (1981). One of them has been assigned tentatively to the fossil anthropoid *Apidium*; the other may belong to any of the larger anthropoids (i.e., *Aegyptopithecus*, *Parapithecus*, *Propliopithecus*). The canal in the subarcuate fossa is absent in sampled extant catarrhines, *Tarsius*, and the isolated petrosals of ?*Apidium* and ?*Aegyptopithecus* discussed by Cartmill *et al.* (1981).

Character 24. Another unambiguous character on the most parsimonious trees that supports platyrrhine monophyly is zygomatic-parietal contact on the sidewall of the skull as seen in side view (Figure 3). In *Tarsius*, living catarrhines, *Aegyptopithecus*, and possibly *Apidium* (Simons, 1959; Fleagle & Rosenberger, 1983), these two bones do not make contact on the sidewall of the skull because the alisphenoid and frontal are interposed between them. However, in *Apidium* the surface of the temporal process of the frontal has a rugose surface suggestive of broken bone (Simons, 1959; Fleagle & Kay, 1987) which could have contained the parietal zygomatic suture, as in platyrrhines (Fleagle & Kay,

1987). This possibility needs to be evaluated on more complete cranial remains.

Relationships of Greater Antillean monkeys

In the most parsimonious trees, the clade consisting of *Callicebus* and the Greater Antillean monkeys is supported by four unambiguously placed characters. They share the derived condition of Character 15, possession of two prominences on the lateral wall of the promontorium. The primitive condition for this character is the presence of a flat surface or a single prominence. The other three unambiguously placed characters are: ventral border of zygomatic arch extending below plane of alveolar border (Character 23, derived from a condition in which zygomatic arch is situated higher on face); mandibular canine root highly compressed (Character 34, derived from a more rounded condition); and alveolus of maxillary canine smaller than that of P^4 (Character 62, derived from reverse condition).

The Antillean clade itself is supported by three unambiguous characters: nasal fossa wider than palate at level of M^1 (Character 25, derived from narrower condition depicted in Figure 10); alveolus of mandibular canine buccolingually smaller than that of P_4 (Character 39, derived from reverse condition), and mandibular M_1 protoconid having bulging buccal surface (Character 53, derived from condition in which feature is absent).

The dyad consisting of *Paralouatta* and *Antillothrix* is supported by six unambiguous characters: M_1 oblique cristid intersects protolophid lingual to protoconid (Character 52, derived from a position directly distal to protoconid); P^4 lingual cingulum projects mesially (Character 68, derived from condition in which cingulum projects directly lingually); P^4 subequal to M^1 in buccolingual dimension (Character 70, derived from condition in which P^4 is smaller); M^1 possesses distinct pericone (Character 75,

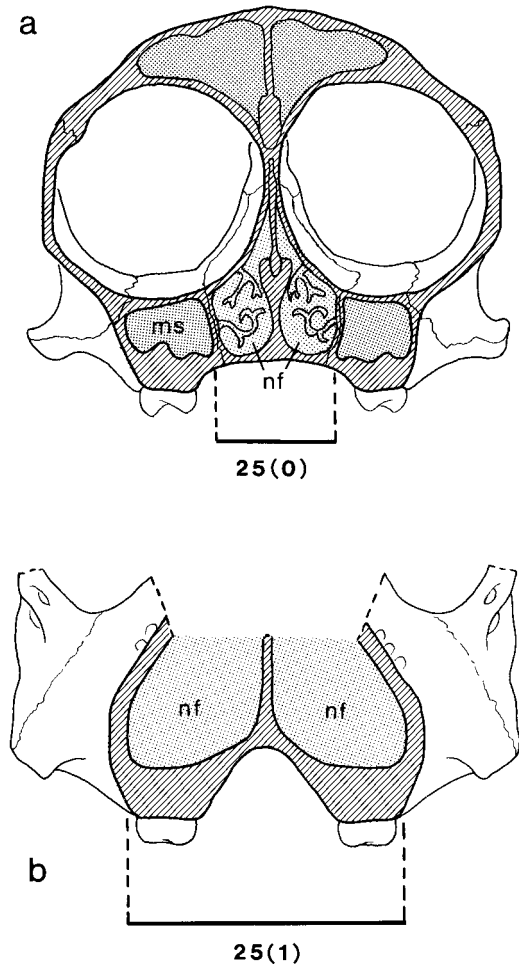


Figure 10. Width of nasal fossa (Character 25) illustrated in (a) *Cebus nigrivittatus* at the level of M^1 , in frontal section (from Hershkovitz, 1977); (b) *P. varonai* at similar level, in imaginary frontal section. In *Cebus*, nasal fossa is narrower than palate between lingual edges of left and right M^1 ; in *Paralouatta*, it is wider (condition shared only with *X. mcgregori*). Features **nf** and **ms** are nasal fossa and maxillary sinus, respectively.

derived from absence of pericone); M^1 post-metacrista slopes distobuccally (Character 73, derived from slope directed distally or distolingually); and M^1 hypocone is located lingually with respect to protocone (Character 74, derived from condition in which this pair of cusps is aligned mesiodistally).

Discussion

At present there is no broadly accepted cladogram of platyrrhine intergeneric relationships. Although there are many reasons for this, it is nevertheless the case that informative morphological characters appear to be relatively hard to find in this group: individual taxa are highly autapomorphic, and published trees contain large amounts of homoplasy.

Rosenberger (1981, 1984), Ford (1986b), Kay (1990), and MacPhee *et al.* (1995) have presented trees that have some features in common. Thus all of these workers recognize 16 living genera, and apportion the majority of them in the same way among three major phylogenetic groupings: Atelinae, including *Ateles*, *Brachyteles*, *Lagothrix*, and *Alouatta*; Pitheciini, including *Pithecia*, *Cacajao*, and *Chiropotes*; and Callitrichinae, including *Callimico*, *Callithrix*, *Cebuella*, *Saguinus*, and *Leontopithecus*. It has proven much more problematic to come to a consensus regarding how the specified groups are related to each other and to the several genera—*Cebus*, *Saimiri*, *Callicebus*, and *Aotus*—that are especially difficult to fit into existing schemes.

Molecular data amenable to cladistic analysis have only been collected since 1993. In the first data set to be published (Schneider *et al.*, 1993), sequences of nucleus-encoded ϵ -globin genes produced highly consistent trees and a highly resolved consensus diagram. However, in that paper the relationships among *Saimiri*, *Cebus*, *Aotus*, and callitrichines remained unsettled, although there were strong indications that these taxa form a clade. Addition of sequences of another gene, the interstitial retinol-binding protein gene (IRBP) intron 1 orthologues (Harada *et al.*, 1995; Schneider *et al.*, 1996) did not resolve this uncertainty. Addition of mitochondrial data (part of the 16 S ribosomal gene and the complete 12 S ribosomal gene) to the

nuclear data set by Horovitz *et al.* (1998) resulted in *Aotus* being positioned as the basal member of a clade otherwise formed by the set ((callitrichines) (*Cebus*, *Saimiri*)), although the support for this topology is weak. The other major clade consisted of atelines and pitheciines, with the latter including *Callicebus* and the pitheciins.

Most branches of the molecular and morphological trees mentioned above are short, except for those supporting the three major groups, atelines (*Ateles*, *Lagothrix*, *Alouatta*, and *Brachyteles*), callitrichines (*Callithrix*, *Cebuella*, *Saguinus*, and *Leontopithecus*) and pitheciins (*Pithecia*, *Cacajao*, and *Chiropotes*). This suggests that a rapid basal radiation of this group of primates occurred, and provides a plausible reason why the topology of their phylogenetic tree is highly unstable. The trees we obtained for New World monkeys in the present study suggest a similar conclusion.

In the present study, retrieved relationships are almost identical to those obtained by Horovitz & Meyer (1997) and Horovitz *et al.* (1998) for morphological characters, despite the addition of three fossil taxa from the Caribbean. Compared to results of other workers, our findings correspond closely to Rosenberger's original analyses, as well as to those obtained with nuclear sequences (Schneider *et al.*, 1993, 1996; Harada *et al.*, 1995) and combined data sets [nuclear and mitochondrial sequences plus morphological data (Horovitz & Meyer, 1997; Horovitz *et al.*, 1998)].

Our results also confirm our preliminary ideas (MacPhee *et al.*, 1995) regarding the cladogeny of Greater Antillean monkeys. Thus, in this study, as in the preceding one, *Callicebus* emerges as the sister group of Greater Antillean monkeys. But whereas previously we considered only the relationships of *Paralouatta* and *Antillothrix* (which remain sister taxa, as before), we now find that parsimony favours the inclusion of *Xenothrix* within this group. We

conclude from this that the monophyly of the Antillean radiation can be considered to be further confirmed, with *Xenothrix* as the basal taxon and *Callicebus* as the mainland sister group.

The chief biogeographical implication of the discovery that Greater Antillean monkeys form a monophyletic group is obvious: it is now parsimonious to assume that only one primate colonization took place from the South American mainland, as opposed to several unrelated events invoked or implied by previous studies. The minimum date for this colonization event is early Miocene, since this is the age of the earliest primate fossil recovered from the Greater Antilles, the Zaza talus. However, the colonization could have taken place well before this, since Paleogene land-mammal fossils have been recovered from Puerto Rico (MacPhee & Iturralde-Vinent, 1995) and Jamaica (Domning *et al.*, 1997).

Acknowledgements

The specimens of *Paralouatta varonai* discussed in this paper were collected between 1988 and 1996 (see Jáimez Salgado *et al.*, 1992; MacPhee *et al.*, 1995), and have been incorporated into the permanent collections of the MNHNH. For various forms of assistance over the years, we are happy to record our grateful thanks to Grupo Espeleológico Pedro Borrás of the Sociedad Espeleológica de Cuba, especially Efrén Jáimez Salgado, Divaldo Gutiérrez Calvache, Rolando Crespo Díaz, and Osvaldo Jiménez Vásquez, and the staff of the MNHNH, especially Manuel Iturralde-Vinent, Stephen Díaz Franco, and Reinaldo Rojas Consuegra. Our thanks also go to Donald A. McFarlane for permitting us to include in our investigation the specimens of *Xenothrix mcgregori* collected by him and the junior author. Clare Flemming also participated in the fieldwork in Cuba and Jamaica. We are additionally grateful to Lorraine

Meeker (photography and Figures 1, 6, and 10) and Clare Flemming (editorial assistance and Figure 3). Finally, we thank John Fleagle and three anonymous reviewers for helpful and perceptive comments on this paper.

References

- Ameghino, F. (1906). Les formations sédimentaires du Crétacé supérieur et du tertiaire de Patagonie avec un parallèle entre leurs faunes mammalogiques et celles de l'ancien continent. *Ann. Mus. Nac. Hist. Nat. ser. III* **15**, 1–568.
- Ashley-Montagu, M. F. (1933). The anthropological significance of the pterion in the primates. *Am. J. phys. Anthropol.* **18**, 158–336.
- Bremer, K. (1988). The limits of amino-acid sequence data in angiosperm phylogenetic reconstruction. *Evolution* **42**, 795–803.
- Buffon, G. L. L. (1767). Histoire naturelle générale et particulière avec description du cabinet du roi [with supplement by M. Daubenton]. Vol. **15**, p. 327.
- Cartmill, M. (1978). The orbital mosaic in prosimians and the use of variable traits in systematics. *Folia primatol.* **30**, 89–114.
- Cartmill, M., MacPhee, R. D. E. & Simons, E. L. (1981). Anatomy of the temporal bone in early anthropoids, with remarks on the problem of anthropoid origins. *Am. J. phys. Anthropol.* **56**, 3–21.
- Domning, D. P., Emry, R. J., Portell, R. W., Donovan, S. K. & Schindler, K. S. (1997). Oldest West Indian land mammal: rhinocerotoid ungulate from the Eocene of Jamaica. *J. Vert. Paleont.* **17**, 638–641.
- Erikson, G. E. (1963). Brachiation in New World monkeys and in anthropoid apes. *Symp. Zool. Soc. Lond.* **10**, 135–163.
- Fick, R. (1911). *Handbuch der Anatomie und Mechanik der Gelenke III*. Jena: Fischer.
- Fleagle, J. G. (1988). *Primate Adaptation and Evolution*. New York: Academic Press.
- Fleagle, J. G. (1990). New fossil platyrrhines from the Pinturas Formation, southern Argentina. *J. hum. Evol.* **19**, 61–85.
- Fleagle, J. G. & Bown, T. M. (1983). New primate fossils from Late Oligocene (Colhuehuapian) localities of Chubut Province, Argentina. *Folia primatol.* **41**, 240–266.
- Fleagle, J. G. & Kay, R. F. (1987). The phyletic position of the Parapithecidae. *J. hum. Evol.* **16**, 483–531.
- Fleagle, J. G., Kay, R. F. & Anthony, M. R. L. (1997). Fossil New World monkeys. In (R. F. Kay, R. H. Madden, R. L. Cifelli & J. J. Flynn, Eds) *Vertebrate Paleontology in the Neotropics*, pp. 473–495. Washington D.C.: Smithsonian Institution Press.
- Fleagle, J. G., Powers, D. W., Conroy, G. C. & Watters, J. P. (1987). New fossil platyrrhines from Santa Cruz Province, Argentina. *Folia primatol.* **48**, 65–77.
- Fleagle, J. G. & Rosenberger, A. L. (1983). Cranial morphology of the earliest anthropoids. In (M.

- Sakka, Ed.) *Morphologie Evolutive, Morphogenèse du Crâne et Origine de L'Homme*, 141–153. Paris: CNRS.
- Ford, S. M. (1986a). Subfossil platyrrhine tibia (Primates: Callitrichidae) from Hispaniola: a possible further example of island gigantism. *Am. J. phys. Anthropol.* **70**, 47–62.
- Ford, S. M. (1986b). Systematics of the New World monkeys. In (D. R. Swindler & J. Erwin, Eds) *Comparative Primate Biology*, 1: Systematics, Evolution and Anatomy, pp. 73–135. New York: Alan R. Liss.
- Ford, S. M. (1990). Platyrrhine evolution in the West Indies. *J. hum. Evol.* **19**, 237–254.
- Ford, S. M. & Morgan, G. S. (1988). Earliest primate fossil from the West Indies. *Am. J. phys. Anthropol.* **75**, 209.
- Goodman, M. (1973). The chronicle of primate phylogeny contained in proteins. *Symp. Zool. Soc. London* **33**, 339–375.
- Goodman, M. (1976). Toward a genealogical description of the primates. In (M. Goodman & E. Richard, Eds) *Molecular anthropology: Genes and proteins in the evolutionary ascent of the primates*, pp. 321–353. New York: Plenum Press.
- Goodman, M., Czelusniak, J. & Beeker, J. E. (1985). Phylogeny of the primates and other eutherian orders: a cladistic analysis using amino acid and nucleotide sequence data. *Cladistics* **1**, 171–185.
- Harada, M. L., Schneider, H., Cruz Schneider, M. P., Sampaio, I., Czeluzniak, J. & Goodman, M. (1995). DNA evidence on the phylogenetic systematics of New World monkeys: support for the sister-grouping of *Cebus* and *Saimiri* from two unlinked nuclear genes. *Mol. Phylogen. Evol.* **4**, 331–349.
- Hershkovitz, P. (1970). Notes of Tertiary platyrrhine monkeys and description of a new genus from the late Miocene of Colombia. *Folia primatol.* **12**, 1–37.
- Hershkovitz, P. (1974). A new genus of late Oligocene monkey (Cebidae, Platyrrhini) with notes on post-orbital closure and platyrrhine evolution. *Folia primatol.* **21**, 1–35.
- Hershkovitz, P. (1977). *Living New World Monkeys (Platyrrhini) with an Introduction to Primates*. Chicago: Chicago Univ. Press.
- Hershkovitz, P. (1981). Comparative anatomy of platyrrhine mandibular cheekteeth dpm_4 , pm_4 , m_1 , with particular reference to those of *Homunculus* (Cebidae) and comments on platyrrhine origins. *Folia primatol.* **35**, 179–217.
- Hershkovitz, P. (1984). More on *Homunculus* dpm_4 and M_1 and comparisons with *Alouatta* and *Stirtonia*. *Am. J. Primatol.* **7**, 261–283.
- Hill, J. P. (1926). Demonstration of the embryologia varia (Development of *Hapale jacchus*). *J. Anat.* **60**, 486–487.
- Hoffstetter, R. (1969). Un primate de l'oligocène inférieur sud-américain: *Branisella boliviana* gen. et sp. nov. *C. r. hebd. Séanc. Acad. Sci. sér. D* **269**, 434–437.
- Horovitz, I. (1995). A phylogenetic analysis of the basicranial morphology of New World monkeys. *Am. J. phys. Anthropol.* (Suppl. 20), 113.
- Horovitz, I. (1997). Platyrrhine systematics and the origin of Greater Antilles monkeys. Ph.D. Dissertation. State University of New York at Stony Brook.
- Horovitz, I. & Meyer, A. (1995). Systematics of the New World monkeys (Platyrrhini, Primates) based on 16S mitochondrial DNA sequences: A comparative analysis of different weighting methods in cladistic analysis. *Mol. Phylogen. Evol.* **4**, 448–456.
- Horovitz, I. & Meyer, A. (1997). Evolutionary trends in the ecology of New World monkeys inferred from a combined phylogenetic analysis of nuclear, mitochondrial, and morphological data. In (T. J. Givnish & K. J. Sytsma, Eds) *Molecular Evolution and Adaptive Radiation*, pp. 189–224. Cambridge: Cambridge University Press.
- Horovitz, I., Zardoya, R. & Meyer, A. (1998). Platyrrhine systematics: A simultaneous analysis of molecular and morphological data. *Am. J. phys. Anthropol.* **106**, 261–281.
- Horovitz, I., MacPhee, R. D. E., Flemming, C. & McFarlane, D. A. (1997). Cranial remains of *Xenothrix* and their bearing on the question of Antillean monkeys origins. *J. Vert. Paleont.* (Suppl. 3), 54A.
- Iturralde-Vinent, M. A. & MacPhee, R. D. E. (in press). Cenozoic paleogeography of the Caribbean Region: Implications for historical biogeography. *Bull. Amer. Mus. Nat. Hist.*
- Jáimez Salgado, E. J., Gutiérrez Calvache, D. G., MacPhee, R. D. E. & Gould, G. C. (1992). The monkey caves of Cuba. *Cave Science* **19**, 25–28.
- Källersjö, M., Farris, J. S., Kluge, A. & Bult, C. (1992). Skewness and permutation. *Cladistics* **8**, 275–287.
- Kay, R. F. (1990). The phyletic relationships of extant and fossil Pitheciinae. *J. hum. Evol.* **19**, 175–208.
- Kay, R. F. & Meldrum, D. J. (1997). A new small platyrrhine and the phyletic position of Callitrichinae. In (R. F. Kay, R. H. Madden, R. L. Cifelli & J. J. Flynn, Eds) *Vertebrate Paleontology in the Neotropics*, pp. 435–458. Washington D.C.: Smithsonian Institution Press.
- Kay, R. F. & Williams, B. A. (1994). Dental evidence for anthropoid origins. In (J. G. Fleagle & R. F. Kay, Eds) *Anthropoid Origins*, pp. 361–445. New York: Plenum.
- Kay, R. F., Madden, R. H. & Guerrero Díaz, J. (1989). Nuevos hallazgos de monos en el Mioceno de Colombia. *Ameghiniana* **25**, 203–212.
- Kay, R. F., Madden, R. H., Plavcan, J. M., Cifelli, R. L. & Guerrero Díaz, J. (1987). *Stirtonia victorae*, a new species of Miocene Colombian primate. *J. hum. Evol.* **16**, 173–196.
- Kinzey, W. G. (1973). Reduction of the cingulum in the Ceboidea. In (W. Montagna, Ed.) *Symp. Fourth Int. Congr. Primatol.*, **3**, pp. 101–127. Basel: Karger.
- Kraglievich, J. L. (1951). Contribuciones al conocimiento de los primates fósiles de la Patagonia. I. Diagnóstico previa de un nuevo primate fósil del Oligoceno superior (Colhehuapiano) de Gaiman,

- Chubut. *Comm. Inst. Nac. Invest. Cien. Nat.* **II**, 57–82.
- Lewis, O. J. (1974). The wrist articulation of the Anthropoidea. In (F. A. Jenkins, Ed.) *Primate Locomotion*, pp. 143–169. New York: Academic Press.
- MacFadden, B. J. (1990). Chronology of Cenozoic primate localities in South America. *J. hum. Evol.* **19**, 7–21.
- MacPhee, R. D. E. (1996). The Greater Antillean monkeys. *Rev. Ciè. (IEB)* **18**, 13–32.
- MacPhee, R. D. E. & Cartmill, M. (1986). Basicranial structure and primate systematics. In (D. R. Swindler & J. Erwin, Eds) *Comparative Primate Biology*, 1: Systematics, Evolution and Anatomy, pp. 73–135. New York: Alan R. Liss.
- MacPhee, R. D. E. & Fleagle, J. G. (1991). Postcranial remains of *Xenothrix mcgregori* (Primates, Xenotrichidae) and other Late Quaternary mammals from Long Mile Cave, Jamaica. In (T. A. Griffiths & D. Klingener, Eds) *Contributions to mammalogy in honor of Karl F. Koopman. Bull. Am. Mus. Nat. Hist.* **20**, 287–321.
- MacPhee, R. D. E., Horovitz, I., Arredondo, O. & Jiménez Vázquez, O. (1995). A new genus for the extinct Hispaniolan monkey *Saimiri bernensis* Rimoli, 1977, with notes on its systematic position. *Am. Mus. Novitat.* **3134**, 1–21.
- MacPhee, R. D. E. & Iturralde-Vinent, M. A. (1995). Earliest monkey from Greater Antilles. *J. hum. Evol.* **28**, 197–200.
- MacPhee, R. D. E. & Woods, C. A. (1982). A new fossil cebine from Hispaniola. *Am. J. phys. Anthropol.* **58**, 419–436.
- Martin, R. D. (1992). Goeldi and the dwarfs: the evolutionary biology of the small New World monkeys. *J. hum. Evol.* **22**, 367–393.
- Napier, J. R. (1961). Prehensibility and opposability in the hands of Primates. *Symp. Zool. Soc. London* **10**, 115–132.
- Orlosky, F. J. (1973). Comparative dental morphology of the extant and extinct Cebidae. Ph.D. Dissertation. University of Washington.
- Pocock, R. I. (1925). Additional notes on the external characters of some platyrrhine monkeys. *Proc. Zool. Soc. London*, 27–42.
- Rimoli, R. (1977). Una nueva especie de monos (Cebidae: Saimirinae: *Saimiri*) de la Hispaniola. *Cuadernos de CENDIA, Universidad Autónoma de Santo Domingo* **242**, 1–14.
- Rivero, M. & Arredondo, O. (1991). *Paralouatta varonai*, a new Quaternary platyrrhine from Cuba. *J. hum. Evol.* **21**, 1–11.
- Rosenberger, A. L. (1977). *Xenothrix* and ceboid phylogeny. *J. hum. Evol.* **6**, 461–481.
- Rosenberger, A. L. (1979). Phylogeny, evolution and classification of New World monkeys (Platyrrhini, Primates). Ph.D. Dissertation. City University of New York.
- Rosenberger, A. L. (1981). Systematics: The higher taxa. In (A. F. Coimbra-Filho & R. A. Mittermeir, Eds) *Ecology and Behavior of Neotropical Primates*, **1**, pp. 111–168. Rio de Janeiro: Academia Brasileira de Ciências.
- Rosenberger, A. L. (1984). Fossil New World monkeys dispute the molecular clock. *J. Hum. Evol.* **13**, 737–742.
- Rusconi, C. (1934). Nuevos restos de monos del terciario antiguo de la Patagonia. *An. Soc. Cient. Argent.* **116**, 286–289.
- Rusconi, C. (1935). Las especies de primates del Oligoceno de Patagonia. *Ameghiniana* **1**, 39–125.
- Saban, R. (1963). Contribution à l'étude de l'os temporal des Primates. Description chez l'Homme et les Prosimiens. Anatomie comparée et phylogénie. *Mém. Mus. nat. Hist. Nat., sér. A, Zoologie* **29**, 1–378.
- Schneider, H., Sampaio, I., Harada, M. L., Barroso, C. M. L., Schneider, M. P. C., Czelusniak, J. & Goodman, M. (1996). Molecular phylogeny of the New World monkeys (Platyrrhini, Primates) based on two unlinked nuclear genes: IRBP Intron 1 and ϵ -globin sequences. *Am. J. phys. Anthropol.* **100**, 153–179.
- Schneider, H., Schneider, M. P. C., Sampaio, I., Harada, M. L., Barroso, C. M. L., Czelusniak, J. & Goodman, M. (1995). DNA evidence on platyrrhine phylogeny from two unlinked nuclear genes. *Am. J. phys. Anthropol.* (Suppl. 20), 191.
- Schneider, H., Schneider, M. P. C., Sampaio, I., Harada, M. L., Stanhope, M., Czelusniak, J. & Goodman, M. (1993). Molecular phylogeny of the New World monkeys (Platyrrhini, Primates). *Mol. Phylogenet. Evol.* **2**, 225–242.
- Schultz, A. H. (1930). The skeleton of the trunk and limbs of higher primates. *Hum. Biol.* **2**, 303–438.
- Schultz, A. H. (1961). Vertebral column and thorax. *Primatologia* **4**, 1–66.
- Setoguchi, T., Watanabe, T. & Mouri, T. (1981). The upper dentition of *Stirtonia* (Ceboidea, Primates) from the Miocene of Colombia, South America, and the origin of the postero-internal cusp of upper molars of howler monkeys *Alouatta*. *Kyoto Univ. Overseas Res. Rep. of New World Monkeys*, 51–60.
- Simons, E. L. (1959). An anthropoid frontal bone from the Oligocene of Egypt: the oldest skull fragment of a higher primate. *Am. Mus. Novitat.* **1976**, 1–16.
- Stirton, R. A. (1951). Ceboid monkeys from the Miocene of Colombia. *Bull. Univ. Calif. Pub. Geol. Sci.* **28**, 315–356.
- Stirton, R. A. & Savage, D. E. (1951). *A New Monkey from the La Venta Late Miocene of Colombia*. Bogotá: Servicio Geol. Nac.
- Williams, E. E. & Koopman, K. F. (1952). West Indian fossil monkeys. *Am. Mus. Novitat.* **1546**, 1–16.
- Wislocki, G. B. (1939). Observations on twinning in marmosets. *Amer. J. Anat.* **64**, 445–483.

Appendix 1

Character list

NOTE: Characters that are multistate and non additive are noted. All others are additive.

- (1) Offspring per birth, number (Wislocki, 1939; Hill, 1926): 0=one, 1=two. *Callithrix*, *Cebuella*, *Saguinus*, and *Leontopithecus* always have dizygotic twins. Singletons occur rarely and are believed to be survivors of dizygotic pregnancies (HersHKovitz, 1977).
- (2) Lumbar vertebrae, number (Erikson, 1963): 0=more than five, 1=five or fewer.
- (3) External thumb (Pocock, 1925): 0=absent or reduced, 1=present. Thumb is nearly or completely absent as an external feature in *Ateles* and *Brachyteles*. In the latter, it is reduced to a very small metacarpal and a single phalanx.
- (4) External tail: 0=absent (not projecting), 1=present. External tail universal in New World monkeys; not projecting (as coccyx) in hominoids.
- (5) Tail, ventral glabrous surface (Pocock, 1925): 0=absent, 1=present. Several genera of New World monkeys display different degrees of prehensility in their tails, which they use either as an additional point of support, to suspend themselves, and/or as a fifth member in locomotion. However, only four genera (*Ateles*, *Lagothrix*, *Brachyteles*, and *Alouatta*) display a patch of naked skin on the distal end of the ventral side of the tail. This feature is readily recognizable on specimens and is presumably related to use in suspension.
- (6) Claws on all manual and pedal digits except hallux (Buffon, 1767): 0=absent, 1=present. Of taxa considered in this study, only five genera possess this feature as defined. Claws and nails are both horny coverings of the terminal phalanges; they differ in that claws are long, sharp, laterally compressed, transversely convex and protruding, whereas nails are broad, blunt, and protrude little or not at all (HersHKovitz, 1977).
- (7) Carpo-metacarpal joint of thumb (Napier, 1961; Fick, 1911): 0=non-saddle, 1=saddle. Catarrhines possess a saddle-shaped joint; all other haplorhines possess conformations that are not saddle-shaped. Napier (1961) described saddle-type articulating surfaces as reciprocally concavo-convex in section and incongruent in at least one plane in joint's mid-position.
- (8) Rib cage, shape (Schultz, 1961): 0=larger dorso-ventrally, 1=larger laterally. Platyrrhines and Old World monkeys differ from hominoids in the transverse shape of their rib-cages: in monkeys, cages are taller than they are wide, in hominoids the reverse obtains.
- (9) Ulnar participation in wrist articulations (Lewis, 1974): 0=present, 1=absent. In most primates except hominoids, ulna articulates with triquetral and pisiform. In hominoids, ulna does not articulate with any wrist bones.
- (10) Sternebral proportions (Schultz, 1930): 0=manubrium shorter than 36% of corpus length, 1=manubrium longer than 46% of corpus length.
- (11) Orbit size (Character 4, MacPhee *et al.*, 1995): 0=smaller than 1.9, 1=larger than 2.1. Size measured as orbit height divided by foramen magnum width; definition of states takes advantage of gap in distribution of ratios.
- (12) Postglenoid foramen (Horovitz, 1997): 0=absent, 1=reduced, 2=large. Coding of this character distinguishes between large foramina, through which interior of braincase is easily visible, and conditions in which foramina are reduced or absent (interior of braincase not visible).
- (13) Tentorium cerebelli, ossification (HersHKovitz, 1977; Horovitz, 1995): 0=absent, 1=present. Tentorium cerebelli presents some degree of ossifica-

- tion in all New World monkey genera (coded as present); it is unossified in all outgroups in which this region could be explored (all extant outgroup taxa used in this study, coded as absent). Degree of ossification is variable, with atelines showing greatest degree and callitrichines and *Saimiri* the least. *Saimiri* is polymorphic (some individuals show slight ossification, others none) (see [Figure 9](#)).
- (14) Middle ear, pneumatization of anteroventral region ([Horovitz, 1997](#)): 0=absent, 1=present. Anterior floor of middle ear in *Callithrix*, *Cebuella*, and *Leontopithecus* displays typical macroscopic consequences of pneumatic activity ([Cartmill et al., 1981](#)). These include formation of septa, small vacuities or cellules, and repositioning of entire sheets of bone such that shape of internal carotid canal is revealed on floor.
- (15) Middle ear, paired prominences on cochlear housing ([Horovitz, 1997](#)): 0=absent, 1=present. Lateral wall of cochlear housing, exposed in medial wall of middle ear cavity, shows variable relief in New World monkeys. In some taxa it is flat or displays a single prominence. In others (callitrichines, *Cebus*, *Aotus*, *Saimiri*, *Callicebus*, *Pithecia*) there is an additional prominence, situated higher and more medially than the first. Also presumably present in *Apidium*.
- (16) Pterygoid fossa, depth ([Horovitz, 1997](#)): 0=deep, 1=shallow. Pterygoid fossa is defined by medial and lateral pterygoid process. In *Paralouatta*, atelines, living pitheciins, *Callicebus*, and callitrichines, medial pterygoid process is greatly reduced. Instead of originating from base of skull, it is restricted to medial side of lateral pterygoid process. As a consequence, pterygoid fossa defined by these processes is shallow, and does not excavate base of skull.
- (17) Canal connecting sigmoid sinus and subarcuate fossa (Character 6, [MacPhee et al., 1995](#)) ([Cartmill, 1981](#); [Horovitz, 1995](#)): 0=absent, 1=present. Present in all examined platyrrhines: *Brachyteles* scored as unknown because status could not be determined in material available (see [Figure 9](#)).
- (18) Vomer, exposure in orbit ([Cartmill, 1978](#); [Rosenberger, 1979](#)): 0=absent, 1=present. Exposed only in *Cebus* and *Saimiri*.
- (19) Ectotympanic, shape (nonadditive): 0=tube I, 1=ring, 2=tube II. Catarrhines and *Tarsius* display a tube-shaped ectotympanic. However, they differ in detail, suggesting nonhomology (scored as “I” and “II”). For discussion, see [MacPhee & Cartmill \(1986\)](#).
- (20) Temporal emissary foramen (Character 7, [MacPhee et al., 1995](#)): 0=present and large, 1=small or absent (see [Figure 3](#)).
- (21) Eyeball physically enclosed ([Martin, 1992](#)): 0=absent, 1=present. Diameter of external orbital aperture is smaller than greatest internal diameter of eyeball in *Callithrix*, *Cebuella*, *Leontopithecus*, and *Saguinus*. This is so because the eyeball is physically enclosed by the external orbital margin ([Martin, 1992](#)).
- (22) Cranial capacity ([Horovitz, 1997](#)): 0=less than 15 cm³, 1=more than 15 cm³. Cranial capacities of New World monkey genera overlap over a wide range of values; however, a gap (reflected in character definition) separates *Callithrix*, *Cebuella*, *Callimico*, *Leontopithecus*, and *Saguinus* (as a group) from other genera. We use this character instead of the more traditionally used body size

- because the former displays an actual gap in its distribution, whereas there is a slight overlap in body size between *Saimiri* and the callitrichines.
- (23) Zygomatic arch, ventral extent (Horovitz, 1997): 0=below plane of alveolar border, 1=above plane of border. In most terminal taxa, entire zygomatic arch is located above tooth row. Some degree of ventral projection may be present, but rarely exceeds level of plane of alveolar border (*Callicebus*, *Aotus*, and *Xenothrix* only).
- (24) Pterion region, contacts (Ashley-Montagu, 1933): 0=zygomatic-parietal, 1=frontal-alisphenoid. In platyrrhines, zygomatic and parietal bones are almost always in contact on external surface of skull in norma lateralis. In all outgroups in which condition is known, frontal contacts alisphenoid (see Figure 3).
- (25) Nasal fossa width (Horovitz, 1997): 0=narrower than palate at level of M^1 , 1=wider. In anthropoids, nasal fossa is generally narrower than width of palate measured between lingual edges of alveoli of M^1 s. By contrast, *Paralouatta* and *Xenothrix* possess unusually wide nasal fossae that (at their maximum width) are broader than palate (see Figure 10).
- (26) Infraorbital foramen, vertical position relative to maxillary cheekteeth in Frankfurt plane (Character 5, MacPhee *et al.*, 1995): 0=above interval between (or caudal to) M^1 and P^4 , 1=above interval between P^4 and P^3 , 2=above (or rostral to) anteriormost premolar (see Figure 3).
- (27) Zygomaticofacial foramen, size relative to maxillary M^1 breadth (Character 1, MacPhee *et al.*, 1995): 0=small, 1=large (see Figure 3).
- (28) Deciduous I_2 , shape (nonadditive) (Horovitz, 1997): 0=bladelike, lingual heel absent, 1=bladelike, lingual heel present, 2=styliform, lingual heel absent. Deciduous I_2 s of *Callithrix* and *Cebuella* are unique among examined haplorhines: they are bladelike, vertically implanted in mandible, with flat lingual and buccal sides (no lingual heel). Deciduous incisors of *Pithecia*, *Cacajao*, and *Chiropotes* also lack a lingual heel, but they are styliform and closely resemble permanent ones. All other taxa have spatulate deciduous and permanent mandibular incisors with lingual heels.
- (29) Relative height of I_1 - I_2 (Rosenberger, 1979): 0= I_1 absent, 1= I_1 lower than I_2 , 2= I_1 - I_2 subequal. *Tarsius* is only taxon in this analysis having a single incisor on each side. In *Callithrix*, *Cebuella*, and *Alouatta*, central incisors are lower than lateral ones; subequal in all other taxa. AMNHM *Brachyteles* specimens not evaluated because teeth too worn to interpret.
- (30) Alignment of I_1 - I_2 (Hershkovitz, 1970, 1977; Rosenberger, 1979): 0=transversely arcuate, 1=staggered. Hershkovitz (1970, 1977) noted that, uniquely in *Callithrix* and *Cebuella*, mandibular incisors are staggered in such a way "that their mesiodistal axes are not linearly aligned but parallel [to] one another in a ranked, *en echelon* spacing" (Rosenberger, 1979: 107). Incisors arrayed in transverse or arcuate arrangement in all other taxa.
- (31) Permanent I_1 - I_2 , shape (Rosenberger, 1979): 0=spatulate, 1=styliform. Permanent mandibular incisors of *Tarsius*, *Callithrix*, *Cebuella*, *Pithecia*, *Cacajao* and *Chiropotes* are mesiodistally compressed and display no lingual heel; in all other taxa they are spatulate, with a lingual heel.
- (32) Mesostyles and distostyles of I_1 - I_2 (Hershkovitz, 1977): 0=absent, 1=present. Mandibular incisors in *Callithrix* and *Cebuella* display small

- mesial and distal cusps flanking major cone.
- (33) Diastema between C_1 and I_2 (Rosenberger, 1979): 0=absent, 1=present. *Pithecia*, *Cacajao*, *Chiropotes*, and *Cebupithecia* all display mandibular diastemata large enough to accommodate maxillary canines when tooth rows are in complete occlusion.
- (34) Root of C_1 shape (Character 11, MacPhee *et al.*, 1995): 0=rounded/suboval, 1=highly compressed.
- (35) Lingual cingulum on C_1 , completeness (Kinzey, 1973): 0=complete, 1=incomplete or absent.
- (36) Lingual crest on C_1 , sharpness (Kay, 1990): 0=rounded, 1=sharp.
- (37) Lingual cingulum on C_1 , mesial elevation of (Horovitz, 1997): 0=not elevated, 1=elevated. In most taxa, lingual cingulum of mandibular canines is mesially elevated (i.e., cingular band is tilted relative to the long axis of the tooth such that it intersects tooth's mesial edge at higher level than its distal edge, usually the lowest point the cingulum reaches).
- (38) Lingual cingulum on C_1 , forming spike on mesial edge of tooth (Horovitz, 1997): 0=absent, 1=present. Lingual cingulum of mandibular canine terminates in a spikelike feature on mesial edge of tooth. In other taxa, this region is flat, not spikelike.
- (39) Buccolingual breadth of alveolus of C_1 compared to P_4 (Horovitz, 1997): 0= C_1 larger than P_4 , 1= C_1 smaller than P_4 .
- (40) Deciduous P_2 , angle subtended by distal portion of mesiodistal axis and postprotocristid (Horovitz, 1997): 0=smaller than 45° , 1=larger than 45° .
- (41) Deciduous P_2 , cross-sectional shape (Horovitz, 1997): 0=rounded, 1=mesiodistally elongated.
- (42) Size of P_2 , relative to P_3 and P_4 (Horovitz, 1997): 0= P_2 smallest in premolar series, 1= P_2 not smallest.
- (43) Deciduous P_3 , metaconid (Kay & Meldrum, 1997): 0=absent, 1=present.
- (44) Protoconid of P_3 , size relative to P_4 protoconid (Horovitz, 1997): 0= P_3 and P_4 protoconids subequal, 1= P_3 protoconid largest.
- (45) Talonid of P_3 (Horovitz, 1997): 0=larger than P_2 talonid, 1=subequal to P_2 talonid.
- (46) Metaconid of P_3 , height relative to protoconid height (Rosenberger, 1979): 0=metaconid absent, 1=metaconid lower than protoconid, 2=metaconid and protoconid subequal, 3=metaconid taller than protoconid.
- (47) Metaconid of P_4 , height relative to protoconid height (Rosenberger, 1979): 0=metaconid lower than protoconid, 1=metaconid and protoconid subequal, 2=metaconid taller than protoconid.
- (48) Hypoconid of P_4 (Kay & Williams, 1994): 0=absent, 1=present.
- (49) Entoconid of P_4 , (Kay & Williams, 1994): 0=absent, 1=present.
- (50) Number of premolars: 0=two, 1=three.
- (51) M_1 projection of distobuccal quadrant (DB complex) (Character 14, MacPhee *et al.*, 1995): 0=not projecting, 1=projecting (crown sidewall hidden in occlusal view).
- (52) M_1 intersection of oblique cristid and protolophid (Character 15, MacPhee *et al.*, 1995): 0=intersects protolophid buccally, directly distal to apex of protoconid, 1=intersects protolophid more lingually, distolingual to apex of protoconid.
- (53) M_1 buccal bulging of protoconid (Horovitz, 1997): 0=absent, 1=present. In both *Paralouatta* and *Xenothrix*, M_1 displays a very convex, bulging buccal surface, especially in the region buccal to the protoconid. When seen from occlusal view, this

- feature makes it seem that the mass of the protoconid and, to a lesser degree, that of the hypoconid, are placed more lingually (“centrally”) than in other platyrrhines.
- (54) M_1 entoconid position (Rosenberger, 1977): 0=on talonid corner, 1=distally separated from talonid corner by sulcus. Rosenberger (1977) noted that *Xenothrix* resembles *Callicebus* and *Pithecia* in displaying a sulcus which separates the entoconid from the post-cristid in such a way that the cusp does not appear to be located on tooth’s distolingual corner. *Alouatta* and *Paralouatta* also display such a sulcus.
- (55) M_1/M_2 buccal cingulum (Kinzey, 1973): 0=absent, 1=present.
- (56) M_2 trigonid/talonid relative height (Kay, 1990): 0=trigonid taller than talonid, 1=subequal.
- (57) M_2 mesoconid (Horovitz, 1997): 0=absent, 1=present.
- (58) M_3/P_4 relative length (Horovitz, 1997): 0= M_3 absent, 1= M_3 shorter, 2=subequal, 3= M_3 longer.
- (59) Molar enamel surface (Rosenberger, 1977): 0=smooth, 1=crenulated.
- (60) I^1 lingual heel (Rosenberger, 1979): 0=absent, 1=present.
- (61) I^2 orientation (Rosenberger, 1979): 0=vertical, 1=proclivious.
- (62) C^1 alveolus size relative to P^4 equivalent (Character 21, MacPhee *et al.*, 1995): 0= C^1 larger than P^4 , 1= C^1 smaller or equal to P^4 . Size is measured as length times width of each alveolus. The two characters reflecting canine size (39 and 62) show different distributions across taxa, and therefore act in ensemble as additive multistate character describing canine size.
- (63) Deciduous P^2 , trigon (Horovitz, 1997): 0=absent, 1=present. Deciduous P^2 is morphologically similar to permanent P^2 in most platyrrhines, except in *Callithrix* and *Cebuella*, which lack a differentiated trigon.
- (64) Deciduous P^3 , hypocone (Horovitz, 1997): 0=absent, 1=present.
- (65) P^3 preparacrista (Horovitz, 1997): 0=absent or vestigial, 1=present.
- (66) P^4 protocone position (Character 23, MacPhee *et al.*, 1995): 0=mesial to widest point of trigon, 1=on widest point.
- (67) P^4 lingual cingulum (Kinsey, 1973): 0=absent, 1=present.
- (68) P^4 lingual cingulum mesial projection (Character 22, MacPhee *et al.*, 1995): 0=absent, 1=present.
- (69) P^4 hypocone (Kay, 1990; MacPhee *et al.*, 1995): 0=absent, 1=present.
- (70) P^4 and M^1 , relative buccolingual breadth (MacPhee *et al.*, 1995): 0= P^4 narrower than M^1 , 1= P^4 subequal to or wider than M^1 .
- (71) M^1 mesostyle/mesoloph (nonadditive) (Kinzey, 1973): 0=absent, 1=mesostyle present, 2=mesoloph present.
- (72) M^1 hypocone/prehypocrista presence (Rosenberger, 1979; Character 30, MacPhee *et al.*, 1995): 0=hypocone and prehypocrista present, 1=hypocone present and prehypocrista absent, 2=hypocone and prehypocrista absent.
- (73) M^1 postmetacrista slope (Character 26, MacPhee *et al.*, 1995): 0=distobuccal slope, 1=distal or distolingual slope.
- (74) M^1 mesiodistal alignment of protocone and hypocone (Character 27, MacPhee *et al.*, 1995): 0=parallel, 1=hypocone lingual.
- (75) M^1 pericone/lingual cingulum (Character 29, MacPhee *et al.*, 1995): 0=absent, 1=lingual cingulum only, 2=distinct pericone on lingual cingulum.
- (76) M^2 hypocone (Rosenberger, 1979; Character 32, MacPhee *et al.*, 1995): 0=absent, 1=present.

- (77) M^2 cristae on distal margin of trigon (nonadditive) (Character 31, MacPhee *et al.*, 1995): 0=cristae form distinct, continuous wall between protocone and metacone, 1=cristae interrupted by fossette or do not form distinct wall, 2=cristae absent or differently organized.
- (78) M^3/P^4 relative mesiodistal length (Rosenberger, 1979; Horovitz, 1997): 0= M^3 absent, 1= M^3 shorter than P^4 , 2= M^3 and P^4 subequal, 3= M^3 longer than P^4 . Mandibular (Character 53) and maxillary third molars sizes relative to P_4/P^4 show different distributions in their character states among taxa scored. Since they provide different information they were both included.
- (79) Maxillary M 's parastyles (Horovitz, 1997): 0=absent, 1=present.
- (80) Ventral flexion of the skull (aiorhynch): 0=absent, 1=present. The angle that the basioccipital forms with the tooth row varies among platyrrhines. The largest angle occurs in *Alouatta*; the next largest in *Paralouatta*, although this species does not actually greatly differ from the average for Platyrrhini. Nevertheless, both were scored as having ventrally flexed skulls.

Appendix 2

Matrix of morphological characters employed to obtain most parsimonious trees whose consensus is shown in Figure 8.

Appendix 2 3

	55	56	57	58	59	60	61	62	63	64	65	66	67	68	69	70	71	72	73	74	75	76	77	78	79	80
1 <i>Tarsius</i>	1	0	0	3	0	0	0	1	0	0	0	?	1	0	0	0	0	2	0	?	1	0	0	3	1	0
2 <i>Leontopithecus</i>	1	0	0	0	0	0	0	0	1	?	0	0	1	0	0	0	0&1	2	1	?	1	0	0	0	1	0
3 <i>Saguinus</i>	1	0	0	0	0	0	0	0	1	0	0	1	1	0	0	0	0&1	2	0	?	1	0	0	0	1	0
4 <i>Callimico</i>	0	0	0	1	0	0	0	0	1	?	0	1	1	0	0	0	1	0	0	?	1	1	0	1	1	0
5 <i>Callithrix</i>	1	0	0	0	0	0	0	0	0	0	0	1	1	0	0	0	0&1	2	0	?	1	0	0	0	1	0
6 <i>Cebuella</i>	1	0	0	0	0	0	0	0	0	0	0	1	0&1	0	0	0	1	2	1	?	1	0	0	0	1	0
7 <i>Aotus</i>	0	0	2	0	0	0	0	0	1	0	0	1	1	0	0	0	0	1	0	?	0&1	1	0	1	0	0
8 <i>Cebus</i>	0	1	0	1	0	0	0	0	1	0	1	1	1	0	0	1	0	1	1	0	0	1	1	1	0	0
9 <i>Cacajao</i>	0	1	1	2	1	1	1	0	1	0	1	1	0	?	0&1	1	0	1	1	0	1	1	1	2	0	0
10 <i>Pithecia</i>	0	1	1	1	1	1	1	0	1	0	1	1	0	?	0&1	0	0	0	1	0	1	1	1	3	0	0
11 <i>Chiropotes</i>	0	1	1	2	1	1	1	0	1	1	1	1	0	?	0&1	1	0	1	1	0	1	1	1	2	0	0
12 <i>Saimiri</i>	1	0	0	1	0	0	0	0	1	1	0	1	1	0	0	1	0&1	1	0	0	2	1	0	1	1	0
13 <i>Alouatta</i>	0	0	0	3	0	1	0	0	1	0	0	0	0	?	0&1	0	2	1	0	0	0&1	1	1	3	0	1
14 <i>Lagothrix</i>	0	0	0	3	0	1	0	0	1	0	0	0	0	?	1	0	0	1	1	0	0	1	0	3	0	0
15 <i>Brachyteles</i>	0	0	0	3	0	?	0	0	?	?	0	0	0	?	0	0	2	1	1	0	0	1	?	2	?	0
16 <i>Callicebus</i>	0	1	0	3	0	1	0	1	1	0	0	1	1	0	1	0	0	0	1	0	1	1	1	2	0	0
17 <i>Ateles</i>	0	0	0	3	0	1	0	0	1	0	0	0	0	?	1	0	0	1	1	0	0	1	0	2	0	0
18 <i>Homo</i>	0	1	0	3	0	0&1	0	0	?	?	0	1	0	?	0	0	0	1	1	0	0&1	1	0	3	0	0
19 <i>Hylobates</i>	0	0	0	3	0	1	0	0	?	0	1	0	0	?	0	0	0	1	1	0	0&1	1	0	3	0	0
20 <i>Cercopithecoids</i>	0	0	0	3	0	1	0	0	?	?	0	1	0	?	0	0	0	1	1	0	0&1	1	2	3	1	0
21 <i>Aegyptopithecus</i>	1	0	0	3	0	1	0	0	?	?	0	1	1	0	1	0	0	1	1	0	0	1	0	3	1	0
22 <i>Cebupithecia</i>	0	?	?	2	0	?	1	0	?	?	1	1	1	0	?	0	0	0	1	0	1	1	?	1	1	?
23 <i>Paralouatta</i>	0	0	0	3	0	0	?	1	?	?	0	1	1	1	0	1	1	0	0	1	2	1	0	2	0	1
24 <i>Anillothrix</i>	?	?	?	?	?	?	?	?	?	?	?	1	1	1	?	1	0	1	0	1	2	1	1	?	1	?
25 <i>Xenothrix</i>	0	1	1	0	0	?	?	?	?	?	1	1	1	0	0	0	0	0	1	0	0	?	?	0	0	?
26 <i>Stirtonia</i>	0	0	0	?	0	?	?	?	?	0	0	0	0	?	1	0	2	1	1	0	1	1	1	?	1	?